AIAA Paper No. 76-3

NASA TECHNICAL MEMORANDUM

NASA TM X-71859

NASA TM X-71859

LIP NOISE GENERATED BY FLOW SEPARATION FROM NOZZLE SURFACES

by W. Olsen and A. Karchmer
Lewis Research Center
Cleveland, Ohio 44135

TECHNICAL PAPER to be presented at
Fourteenth Aerospace Sciences Meeting
sponsored by the American Institute of
Aeronautics and Astronautics
Washington, D.C., January 26-28, 1976

LIP NOISE GENERATED BY FLOW SEPARATION FROM NOZZLE SURFACES

W. Olsen and A. Karchmer
Lewis Research Center
National Aeronautics and Space Administration
Cleveland, Ohio

Abstract

Flow separation from nozzle surfaces can be a source of significant noise in addition to the jet noise. When no flow separation region exists only jet noise is observed at every angle, for velocities down to 120 m/sec, with both low and high levels of initial turbulence. Intense nearly periodic turbulence and noise is caused by flow separation from the thin core nozzle lip of a coaxial nozzle. This can be described by a combination of aeolian tone and trailing edge noise theory. Noise caused by flow separation from the surfaces of other nozzle geometries has somewhat different characteristics.

Introduction

There are additional sources of noise, other than jet noise, that are associated with the flow through a nozzle. One, herein called classic lip noise, was reputed to be caused by turbulent flow passing over one side of the lip of a single stream nozzle.[1,2] Another source of additional noise is due to flow separation off the surfaces of various nozzle geometries. Some examples, which were described very briefly in Ref. 3, are flow separation off the plug of a plug nozzle and flow separation off the core nozzle lip of a coaxial nozzle. In the latter case, a thin flow separation zone occurs downstream of the core nozzle lip which causes intense high frequency noise. Fig. 1 (taken from Ref. 3) shows an example of flow separation noise from a model-scale coaxial nozzle. The flow separation region that occurs downstream of the 0.25 cm thick blunt core nozzle lip of this coaxial nozzle caused the intense narrow band high frequency noise that is as much as 20 dB above the jet noise. This type of additional noise makes the determination of pure jet noise from a model nozzle more difficult as shown in Refs. 4 and 5. Since coaxial and other nozzle shapes are used on aircraft engines, flow separation is also a potential engine noise source.

The objective of this study is to present the results of a series of experiments performed at the NASA Lewis Research Center to investigate flow separation and classic lip noise in much more detail than presented previously[3] and thereby aid in understanding this area of aeroacoustic noise generation.

Several types of nozzle-lip configurations were used to study the high frequency noise generated by small regions of flow separation at the nozzle lip. These included coaxial nozzles, and circular and slot nozzles with splitter plates. The splitter plate geometry was used extensively in these experiments because geometrical variations of the lip (e.g., thickness and span) and turbulence measurements were more easily accomplished than with a coaxial nozzle configuration. The jet flow velocity was varied and far field noise was measured for all nozzle-lip geometries (coaxial and splitter plate). The effect of a velocity difference across the lip of the coaxial nozzle and the splitter plate on the far field noise was also measured. Finally, an effort was made to find means to reduce the high frequency noise caused by flow separation at the lip.

There is no specific theory that applies to the additional noise caused by flow separation from the thin lip of a coaxial nozzle or splitter plate. Therefore, available theories for simple geometries that have somewhat similar acoustic characteristics are adapted to these geometries and compared to the data.

Flow separation can occur off the surfaces of other nozzle shapes and cause additional noise. The characteristics of this additional noise may be somewhat different than the noise caused by flow separation from a thin lip. A few examples are given of flow separation noise from varied nozzle shapes (e.g., plug, orifice, mixed flow coaxial and suppressor nozzles).

Finally, two single stream nozzle geometries (with no flow separation), which had low and high initial turbulence levels, respectively, where run over a range of subsonic velocities from 120 to 300 m/sec. The acoustic spectra for these nozzles were studied near the upstream axis, where theory indicates classic lip noise should dominate, in order to determine if classic lip noise can be observed relative to jet noise.

Apparatus and Procedure

Acoustic Tests

Flow system and valve noise quieting. Two similar test rigs of different size were used to obtain the jet noise data in this paper. Each system conceptually looked like the small rig shown in Fig. 2. The small rig consisted of the following (proceeding downstream): a 10 cm flow control valve; a valve noise quieting section; a long straight run of 10 cm pipe; and finally the test nozzle. The first valve noise quieting element was a perforated plate. Downstream of that was a large volume no-line-of-sight muffler. The rig used for the larger nozzle data (i.e., 10 cm nozzles and larger) was one line of the coaxial nozzle rig described in Ref. 4, which used larger but similar flow lines and hardware.

None of the nozzle jet noise data reported herein were affected by internal valve noise, either through the nozzle exit or by direct radiation through the pipe, which was wrapped with fiberglass and lead vinyl insulation.

Acoustic instrumentation and data analysis. The noise data were measured outdoors with either of two types of semicircular microphone arrays that were centered on the nozzle exit. Condenser microphones (1.27 cm) with windscreens were used with each. Each array had a microphone radius of about

50 nozzle diameters to assure that they were well into the far field for jet noise. The data were taken either with a vertical or horizontal semicircular microphone array (shown in Fig. 2), with open cell acoustical foam on the ground. Either array resulted in free field noise data for frequencies above 200 Hz. Background noise had an effect upon the data below about 400 Hz only when the low frequency noise level was very low.

The data were measured by 11 microphones on a semicircle of 3 or 4.6 meter radius. The microphones were more closely spaced (10^o to 15^o intervals) near the nozzle jet than in the upstream quadrant (20^o to 30^o intervals). In all arrays, the polar angle $\theta_i = 0^o$ corresponds to the nozzle inlet.

Noise data were taken at each microphone location for each run condition. The noise data were tape recorded for subsequent narrowband analysis, and also analyzed directly by an automated one-third octave band spectrum analyzer. Both analysis methods determined sound pressure level spectra, SPL, referenced to 2×10^{-5} N/m^2. The one-third octave band SPL spectra reported were corrected for the small atmospheric attenuation (less than 1 dB) and background noise (less than 3 dB); so that the data are lossless and free of background noise. The results were integrated to obtain the overall sound pressure level, OASPL, and the sound power level spectrum, PWL, as described in Ref. 4. Data for the additional noise due to flow separation (SPL_c and $OASPL_c$) were computed from the 1/3 octave SPL spectra by removing the small jet noise contribution. The reported narrow band spectra were not corrected for the small contributions of atmospheric attenuation, background noise, and jet noise.

The condenser microphones were calibrated before and after each day of testing with a standard piston calibrator (calibration tone of 124 dB at 250 Hz). The third-octave band analyzer was periodically calibrated and checked with a pink noise generator. Considering the microphone calibrations, periodic checks of the data system, and the data averaging, it was determined that the 1/3 octave band data are repeatable from day to day to within a $1\frac{1}{2}$ dB band for the broadband type data and within about a 3 dB band for the narrow band noise data. Most of the directly compared data were taken on the same day, so that these data were repeatable to about half the above dB bands.

The quality of the data can be summarized as follows. The data are repeatable, and far and free field above about 200 Hz. The data are unaffected by background or valve noise down to 60 m/sec for frequencies above 400 Hz as required for the high frequency lip noise experiments; and down to 120 m/sec for the broadband experiments.

Test nozzles. Sketches of the nozzles that were extensively tested herein are shown on Fig. 3. Other nozzles are sketched on the figures containing the applicable data. The nozzles shown in Fig. 3(a) have flow on both sides of a splitter plate. Circular nozzles (7.6 and 10 cm diam.) and slot nozzles (1.9 cm height with 13 and 46 cm widths) enclosed the plates. The splitter width, w, was varied within the 46 cm wide slot nozzle, over a range of width of from 2.5 to 41 cm. Splitter plate thicknesses (t) of 0.16, 0.32, 0.64, and 1.28 cm were tested. Most tests of the above tests involved partial span splitter plate configurations. The velocity ratio across the splitter plate (VR = low velocity/constant high velocity) was varied by restricting the flow through the low velocity side of the full span splitter plate configuration with layers of fine screening and felt. In Fig. 3(a) sketches of the lip and variations tested are also shown. The splitter plates were long enough that their leading edge and any supports were in the inlet pipe where the velocity is less than a quarter of the jet velocity. The exit velocity was uniform across the nozzle. The displacement boundary layer thickness at the nozzle exit end of the splitter plates was less than $3\frac{1}{2}$ percent of the thickness of the thinnest plate tested.

Each nozzle of the coaxial nozzle configuration (Fig. 3(b)) was supplied air independently so that the velocity ratio (VR = outer nozzle velocity/core nozzle velocity = V_o/V) was readily varied while holding the core velocity, V, constant. In most tests these nozzles were coplanar. The core nozzle lip was 0.32 cm thick. In one test the core nozzle lip was lengthened, while in another the outer nozzle was extended.

The next group of test nozzles generate flow separation noise from nozzle surfaces other than thin lips. These nozzles include several plug nozzles, a thick plate orifice, and a mixed flow coaxial nozzle. Sketches of these geometries are shown on the appropriate data figure in the report.

The last group of test nozzles shown in Fig. 3(c) were used to evaluate whether classic lip noise exists as a noise source in addition to jet noise for the practical jet velocities (e.g., greater than 120 m/sec). The first nozzle had a low initial turbulence (measured at the nozzle exit plane) of less than 1/2 percent and a uniform velocity profile. The second nozzle had a long lip pipe that causes a highly turbulent (about 10 percent near the pipe wall) parabolic velocity profile at the exit plane of the nozzle.

Test procedure. The far field noise data taken for the nozzles described in Fig. 3 consisted of 1/3 octave band SPL spectra for all cases and narrow band spectra for most cases. The acoustic data were taken over a maximum velocity range of 60 to 300 m/sec and at ambient temperature. The velocity was varied over nearly the maximum range for most of the configurations shown on Fig. 3. Span and plate thickness were primarily varied with the partial span splitter nozzle, while velocity ratio was varied with the coaxial nozzle and full span plate in a circular nozzle.

Turbulence Tests

Flow system. The flow system used for the turbulence measurements (proceeding downstream) consisted of: a flow control valve, a 7.6 cm diameter plenum tank (with screens and felt filters to reduce any large scale turbulence and remove particulate matter), and finally the test nozzle. The total pressure and temperature in the plenum were monitored with manometers and a thermocouple. The data was taken with the 7.6 cm convergent nozzle and splitter plates that were used in the

acoustic tests previously described.

Instrumentation and procedure. The turbulence data were taken with a hot wire probe. The wire was 0.00038 cm diameter tungsten with an active sensor length of 0.127 cm. The hot wire signal was fed to a TSI model 1050 anemometer and the a.c. portion of the anemometer output recorded on an FM tape recorder. The time response of the hot wire system was flat to 20 kHz. Linearization was not deemed necessary. The tape recorded a.c. signal was then processed through a constant band width spectrum analyzer to obtain the turbulence spectral density plots.

The hot wire probe was mounted on a 3 axis positioner with positioning accuracy to 0.0025 cm. The wire position was referenced from the center of the upper edge of the plate. The turbulence spectra and intensity of the axial velocity component, u, were measured. Measurements were made up to mean velocities of 182 m/sec, without damaging the wire.

The hot wire system was calibrated using the core of the jet prior to each day's running, with the velocity computed directly from the nozzle total temperature and pressure, ambient pressure, and assuming isentropic expansion.

Results and Discussion

This study is concerned with sources of non-internal noise other than jet noise, that can be associated with flow through a nozzle. The primary emphasis of this paper is devoted to the noise generated by flow separation caused by flow on both sides of thin nozzle lip surfaces. In the first part of the first section the noise and turbulence measured for nozzles with thin splitter plates will be discussed. Following that, the noise caused by flow separation off the thin core nozzle lip of the important coaxial nozzle will be described. These data will be explained in terms of an analytical model. A few examples of flow separation noise from other nozzle surfaces are then reported in the second section. The paper ends with a discussion of classic lip noise, where noise has been reputed to be generated by turbulent flow passing over one side of the nozzle lip in the absence of flow separation.

Noise from Flow Separation Off Thin Nozzle Lips

Nozzles with Splitter Plates

The nozzles with a splitter plate (Fig. 3(a)) are considered before the coaxial nozzle because more extensive noise measurements and all the turbulence measurements were taken for that geometry. In any event, it will be shown that the results for these geometries are essentially similar.

Full compared to partial span plates. Both partial and full span splitter plates geometries were tested. The full span plate edge touches the nozzle, while flow passes all around the partial span plate. The noise produced by a partial span splitter plate that does not touch the nozzle (0.32 cm gap) is compared in Fig. 4 to one of slightly wider span that does touch. Two splitter plate thicknesses are used in this comparison. It is apparent that the results are the same for the 0.32 cm thick plate. With the 0.64 cm thick plate, however, the full span plate does not generate significant flow separation lip noise compared to the partial-span plate. The same result occurred at a velocity of 152 m/sec. The lower level of noise with the thick (0.64 cm) full-span plate may be due to the fact that air can more readily flow into the thicker low pressure flow stagnation region from the outside at the edge, which would affect the noise producing eddy structure. To avoid this difficulty, the data that follows will be taken with partial-span splitter plates, whereever a full-span splitter plate is used the plate will be thin (0.32 cm).

Effect of velocity. - Narrowband spectra of flow separation lip noise at $\theta_i = 100^o$ from the inlet are shown in Fig. 5 for a range of jet velocities, at a velocity ratio across the plate (VR) of 1.0. The flow separation zone occurs in the wake of a 0.32 cm inch thick, blunt ended, partial span, splitter plate. The data in Fig. 5 indicate that the thin flow separation zone generates a relatively high frequency narrowband noise that is about 20 dB above the broadband jet noise. Experience gained in previous jet and surface noise experiments has shown that feedback tones generally can be eliminated by probing around and in the flow. The tonelike noise shown in Fig. 5 was not affected by this approach, therefore this noise is probably not due to feedback.

One third octave band lossless data were also taken and the generally negligible contribution of the broadband jet noise was removed, which resulted in the noise due only to flow separation at the lip (SPL_c and $OASPL_c$). These quantities will be used in several figures to follow. The variation of the $OASPL_c$ with velocity for the plate thickness (0.32 cm) used in Fig. 5 is plotted on Fig. 6 as open circles. The data follows the V^6 power law of a dipole noise source. The data for other plate thicknesses will be discussed in the next section.

Effect of plate thickness. Narrowband spectra at 91 and 244 m/sec and VR = 1 for several partial splitter plate thicknesses are shown on Fig. 7. As the plate gets thicker the width of the spectrum for the lip noise gets narrower and the level drops. The 1.28 cm thick plate generates almost periodic (i.e., very narrow width) noise of low level. The 0.16 cm thick plate has a broader spectrum and the level is somewhat lower than that of the 0.32 cm plate. The level of the noise, in terms of the $OASPL_c$, is also shown in Fig. 6; the maximum level occurred for the 0.32 cm thick plate. The thin plate (0.16 cm) has slightly lower levels while thicker plates have much lower levels. The $OASPL_c$ for the 1.28 cm plate is not shown on Fig. 6 because the level is too low, comparable to the level of the jet noise. The spectra on Fig. 7 are for $\theta_i = 100^o$ but the same spectra occurred at other angles.

Radiation pattern. The flow separation noise polar radiation patterns, or variation of $OASPL_c$ with θ_i, are plotted on Fig. 8 for the same velocities and nozzle-lip configuration of Fig. 5. Examination of the narrow band spectra at various θ_i showed that the frequency and spectral shape of the flow separation noise was the same for all θ_i. Fig. 8 indicates that the peak $OASPL_c$ occurred between 100^o and 120^o from the inlet. Refraction of this high frequency noise causes much of the rapid fall off for $\theta_i > 120^o$, especially at high

velocity. The shape of the radiation pattern was unaffected by changes in plate thickness.

The splitter plate geometry cannot result in axisymmetric noise. Fig. 9 contains a plot of the azimuthal variation of the $OASPL_c$ at a polar angle of $\theta_i = 90^o$ for a 0.32 cm thick splitter plate (plate width/thickness, 23) and a velocity of 152 m/sec. It is apparent that the level decreases from the maximum level at $\phi = 0^o$ (plane through nozzle centerline axis and perpendicular to the plate) approximately according to $\cos^2\phi$. The shape of the polar radiation pattern ($OASPL_c$ $<\theta_i>$ is independent of ϕ.

Frequency of the noise. In this section the dependence of frequency on plate thickness and velocity will be examined. The narrow band spectra (Figs. 5 and 7) usually have a single dominant peak; but sometimes there are two dominant peaks or a fairly flat peak. The peak frequency, f_p, will be taken as the frequency of the single peak if one exists, or the frequency in the center of two equal peaks or a flat peak. In Fig. 10, data for f_p is plotted as a function of V/t. These data were taken over a range of velocities, V, for several plate thicknesses, t, of the partial span splitter plate configuration. The data approximately collapse about a line defined by the following Strouhal relation.

$$f_p = S_t(V/t) \qquad (1)$$

Examination of the data for each thickness has shown that f_p is very nearly proportional to V. The inverse proportionality of f_p with thickness is less exact as evidenced by the width of the band of data that is ±10 percent of f_p wide for the same geometry data (open symbols). A Strouhal number of $S_t = 0.22$ fits the partial-span splitter plate data adequately. The data were taken at $\theta_i = 100^o$ and $\phi = 0^o$, but as shown previously these results apply at all angles θ_i. There was no Doppler shift in frequency of the peak noise with angle, as was expected with this noise source that is stationary with respect to the microphone.

Effect of splitter span width and scale. Slot nozzles with 0.32 cm thick partial-span splitter plates were employed to determine the effect of splitter plate width. Fig. 11(a) shows narrowband spectra at $\theta_i = 100^o$ and V = 91 m/sec for a range of partial-span splitter plate widths. As the width, w, increased from 2.5 to 40 cm, the peak frequency of the noise decreased slightly from about 9.5 kHz to about 8.5 kHz. The level of the peak noise increased significantly (about 20 dB). The Strouhal number for the 40 cm plate, over a large range of velocity, was 0.28. The same spectral trends occurred at all θ_i. A weak harmonic is evident at 10 kHz in the data for large spans. Previously discussed data rarely exhibited a harmonic, possibly because the span was not large.

The shape of the radiation pattern is also independent of w. The variation of the level ($OASPL_c$ at $\theta_i = 100^o$) with width, w, is plotted on Fig. 11(b) for the preceding data on Figs. 6 and 11(a); and also data taken with another slot nozzle. The same curve shape has been put through the data taken at both velocities (91 and 152 m/sec). At large plate widths (w > 10 cm) the level of the noise is proportional to w, but for small widths (w < 5 cm) the level changes much more rapidly. This suggests that the level of the lip noise for a coaxial nozzle would be proportional to the diameter of the core nozzle, for core nozzles having a circumference larger than about 10 cm (i.e., 3 cm diam.). Jet noise is proportional to the square of the diameter. Therefore, it can be expected that flow separation lip noise (proportional to the diameter) would be less significant (relative to the jet noise) for the large coaxial nozzle of an engine than for a small scale model of that nozzle.

Effect of velocity ratio. In Fig. 1, taken from Ref. 3, it is clearly shown that for coaxial nozzles the velocity ratio, VR, across the core nozzle lip has a strong effect on flow separation lip noise. When the velocity ratio was below 0.5 the lip noise was less than the broadband jet noise. The effect of velocity ratio on the flow separation lip noise from a splitter plate nozzle is now discussed. Because a single air line was used in the splitter experiments, the velocity ratio across the splitter plate was changed by using appropriate layers of screens and felt to restrict the flow on one side of the plate. The data for splitter plates with varying velocity ratio, VR = low velocity/fixed high velocity, are shown in Fig. 12 in terms of the SPL as a function of frequency. The splitter plate results (Fig. 12) are qualitatively the same as the coaxial nozzle results of Fig. 1 in the sense that the lip noise decreases rapidly as the VR decreases.

Methods to reduce lip noise. The previous results suggest that flow separation lip noise could be eliminated as a significant additional noise source by two methods. In one method, a thick blunt lip (e.g., $t \geq 1.28$ cm) can be used, as shown by Fig. 7, to reduce the lip noise to a manageable level. In the second method, the blunt lip would be made thin enough so that the resulting flow separation noise is of such a high frequency that it is beyond the range of interest.

Additional means were also tested, which may reduce the lip noise. These configurations, which are shown on Fig. 3(a), involved changes to the downstream end of a 0.64 cm thick partial-span splitter plate. In one case, the end was tapered gradually to a sharp edge. In another case air flowed (i.e., vented) through the blunt end at 85 percent of the jet velocity. Both of these methods effectively eliminated the flow separation lip noise (or moved it to very high frequency) so that only the nozzle alone jet noise spectra was measured. The wedge of fine screening was not effective in reducing the lip noise.

Turbulence data. A number of turbulence measurements were taken to determine the characteristics of the flow downstream of the splitter plate. The axial velocity perturbation was measured downstream of the same 7.1 cm wide partial-span splitter plate nozzle configurations used for the previous acoustic tests (Figs. 5 to 8, 10). Many traverses were made across and axially along the flow separation region of the plates. It was found that the maximum turbulence occurred for all plates (0.16 through 1.28 cm thick) at approximately two thicknesses (x = 2t) downstream of the edge of the plate (y = 0 and y = -t).

In Fig. 13 a plot is shown of axial turbulent velocity perturbation spectra measured for several

traverse (y) locations at $x = 2t$, for a $t = 0.32$ cm thick plate. The axial velocity perturbation, u', is plotted as $10 \log_{10}(u')^2$. Notice that the spectra at the edge of the plate ($y = 0$) has a strong primary peak. The primary peak weakens and a secondary peak of twice the primary frequency gets stronger at the center of the plate ($y = -t/2$). It is likely that this is caused by the eddies being released alternately at the top and bottom edges of the plate. With the wire at the edge of the plate ($y = 0$) only the eddies released at that edge are picked up at the primary frequency. But the wire, when at the center of the plate ($y = -t/2$), is also affected by the eddies alternately released on both sides of the plate. Therefore, the primary frequency and also double the primary frequency are observed. Movies and an analysis that describe the periodic eddy flow from a splitter plate were discussed in Ref. 5. The description of the flow is essentially the same as described above. The above flow description is also the same as would be measured downstream of a stationary small diameter cylinder,[6] where the alternate periodic shedding of vortices into the wake produces an oscillating force at the primary frequency. The oscillating lift force acting on the cylinder is responsible for the aeolian tone noise that is observed. The frequency of the noise tone is the same as the primary vortex shedding frequency.

The effect of velocity is shown on Fig. 14 where the velocity was varied from 24 to 186 m/sec. A 0.32 cm thick partial span splitter plate was used here with the wire located two thicknesses downstream of the plate edge ($x = 2t$, $y = 0$). Notice that the turbulence spectra becomes only slightly broader at the higher velocities. The level of the peak of the u' spectra remained nearly constant as the velocity was increased. The turbulence intensity, noted in the table on Fig. 14, increased only slightly with velocity. The increase would even be smaller if the small contribution of the broadband signal had been filtered out. The Strouhal number for the turbulence peaks is $S_t = 0.22$, which is the same value found for the acoustic data for this nozzle-lip configuration (Fig. 10). These results are consistent with the description of the aeolian tone theory found in Ref. 6.

In Fig. 15 the turbulence spectra measured at $x = 2t$ and $y = 0$ is plotted for $t = 0.16$, 0.32, and 0.64 cm thick partial-span splitter plates at $V = 87$ m/sec. The turbulence spectra becomes more narrowband as the plate gets thicker. This turbulence essentially disappeared with the 1.28 cm plate (i.e., turbulence level at least 20 dB down) so that it is not shown in Fig. 15. The shape of the turbulence spectra (Fig. 15) are about the same as for the acoustic results (Fig. 7(a)). The Strouhal number for the turbulence data (0.22) agrees with the Strouhal number for the acoustic data (0.22, Fig. 10).

The effect on the turbulence of the velocity ratio, VR, across the plate is discussed below. The turbulence spectra were measured on both sides of the plate ($y = 0$ and $y = -t$) at $x = 2t$ for a 0.32 cm thick full span splitter plate (Fig. 16). The velocity on one side of the plate was held at 97 m/sec, while the other side was restricted by layers of felt to achieve a range of velocity ratios, VR. The turbulence spectra on each side of the plate changed together as the velocity ratio decreased (Fig. 16). The turbulence level decreased and the spectra becomes more broadband when the VR was less than 0.5. The flow visualization movies and analysis reported in Ref. 5 also indicated that the eddies leaving the lip become much less periodic (i.e., spectra more broadband) as the velocity ratio falls below 0.5. This reduction in periodicity and turbulence level would certainly reduce the level of the lip noise. The change in level and the frequency shift is similar to the results seen in the acoustic data (Fig. 12).

Coaxial Nozzle

This section discussed flow separation noise from a blunt, thin core nozzle lip of a coaxial nozzle. The data for the coaxial nozzle lip are essentially similar to the splitter plate lip except that coaxial nozzle flow separation noise is axisymmetric; and the turbulent eddy structure is somewhat different for a circular lip.

Effect of velocity. The narrowband spectra for flow separation noise from a 0.32 cm thick core nozzle lip is shown on Fig. 17 for several core velocities, V. Comparison of these spectra with those obtained for an 0.32 cm thick partial splitter plate (Fig. 5) indicate very similar results. The Strouhal number for these data is 0.20 (Fig. 10) which is close to the 0.22 value for the splitter plate data in Fig. 10. The spectral data apply to all angles, θ_i. The $OASPL_c$ for these data are plotted on Fig. 18 together with the data for splitter plate from Fig. 6. The data have been scaled to the same microphone distance and environmental temperature. It is apparent that the same V^6 trend occurs with the coaxial nozzle as it did with the partial-span splitter plate, but the level is higher. According to Fig. 11(b) all of the configurations used in Fig. 18 have a large enough width (or circumference) for the noise level to be nearly proportional to the width. From Ref. 7 it is expected that the level of the noise from a 1 cm wide plate lip (at $\phi = 0$) would be the same as a circular lip whose circumference is 2 cm. All cases on Fig. 18 turn out to be with 1/2 dB of being the same equivalent width. The coaxial nozzle flow separation noise is about 9 dB higher than the splitter data on Fig. 6. This implies that the turbulence eddy structure is somehow different than it is for the splitter plate geometry, in so far as it affects the level of the noise.

The noise radiation patterns, or the variation of $OASPL_c$ with θ_i, is plotted on Fig. 19 for several velocities. The radiation pattern curves that were drawn through the splitter data on Fig. 8, have also been put through the data at 90^o angle in Fig. 19. This permits a comparison of the shape of the radiation patterns for the coaxial and splitter lip geometries. The shape of the patterns are almost the same.

Effect of velocity ratio. In Fig. 20, narrowband spectra are shown that were obtained for several outer nozzle/core velocity ratios ($VR = V_o/V$, between 1 and 0), with a constant core velocity, V, of 152 m/sec. The level drops rapidly as the outer nozzle velocity is lowered from a velocity ratio of one. Below a velocity ratio of about 0.5 the flow separation lip noise cannot be discerned from the broadband jet noise of this case. The peak frequency shifts slightly between $VR = 1.$ and 0.8;

below VR = 0.8 it stays constant. The same results occurred at all angles.

Noise contours near the nozzle. An array of five 0.64 cm microphones were placed at several locations in the vicinity of the nozzle, but outside of the flow. Constant noise level contours of the flow separation lip noise near the nozzle were located with this arrangement. The contours shown on Fig. 21 were obtained with an 0.32 cm thick lip at a core velocity of 152 m/sec and VR = 1. The lip noise for this case (from Fig. 17) peaks between 9 and 10 kHz. Since the flow separation region (i.e., source of the lip noise) is very compact and the noise is of very high frequency, it should be possible to use the noise contours to locate the noise source. The contours do seem to indicate that the lip noise is radiating from the core nozzle lip. The previous acoustic and turbulence data contained in this report, where changes were made in the flow and geometry at the lip, also strongly indicate that flow separation from the core nozzle lip is the source of the noise.

Effect of outer nozzle extension. In Fig. 22 the acoustic characteristics of an extended outer nozzle are compared to a coaxial nozzle with coplanar nozzles. The outer nozzle is extended four outer nozzle diameters downstream ($L_o/d_o = 4$) from the core nozzle. The core nozzle has a 0.32 cm thick lip. This case is compared to the coplanar coaxial nozzle ($L_o/d_o = 0$) at the same core exit plane velocities. Flow separation from the core nozzle lip again causes a nearly narrowband spectrum. The frequency of the tone was independent of L_o/d_o and θ_i. The radiation pattern changed slightly because the noise is generated in a duct. The lip noise level at $\theta_i = 105^o$ is somewhat lower for the extended outer nozzle geometry compared to the coplanar result primarily because the $OASPL_c$ for the $L_o/d_o = 4$ case reached its peak further downstream (at $\theta_i = 120^o$) than for the coplanar case (at $\theta_i = 105^o$). It can be assumed that, except for the duct acoustics, this noise source is unaffected by the outer nozzle duct.

Correlation of the Data

There is no specific theory that applies the lip noise caused by flow separation from a thin lip. However, equations that describe the data for this geometry might be generated from the basic theories for simple geometries described in Ref. 8. The turbulent flow characteristics, geometry and previous acoustic results suggest that two noise sources are involved. One source has characteristics that are similar to the noise produced by air flowing over a small cylinder. The coherent periodic shedding of eddies in the wake of the cylinder results in a fluctuating lift force (drag neglected) that produces a discrete aeolian tone with a lift-dipole radiation pattern ("dipole noise"). The other source has the radiation pattern that results for a semi-infinte plate[1] when there is high frequency turbulence (nearly periodic in this case) very near the edge of the surface ("trailing edge noise").

These two acoustically independent, nearly periodic noise sources are combined according to the following relationship for the level of the lip noise caused by flow separation from blunt thin nozzle lips.

$$OASPL_c = 10 \log_{10}\left\{\left(\frac{\rho_o}{c_o}\right)^2\left(\frac{w\xi}{R^2}\right)\Phi \times \left[\frac{KV^6 \sin^2\theta_i}{\left(1 + \frac{V}{c_o}\cos\theta_i\right)^4} + V^5 \cos^2(\theta_i/2)\right]\right\} + C \quad (2)$$

"dipole noise" "trailing edge noise"

The velocity, V, is the larger velocity at the lip when VR ≠ 1. The lip width, w, is the width of the splitter plate, or the core nozzle circumference for the coaxial nozzle. According to the aeolian tone theory the term ξ could be considered to be a correlation length. In the absence of direct measurements, ξ must be evaluated from the previous data. These data show that ξ is a function of the lip geometry (thickness (t), width (w), and shape (circular or splitter)). It is also a function of the local flow at the lip (velocity ratio across the lip (VR), initial turbulence, and a weak function of velocity). The term Φ is equal to 1/2 for the axisymmetric lip noise of a coaxial nozzle, while $\Phi = \cos^2\phi$ for a splitter plate. The term C is a constant.

The frequency of the peak of the tonelike (nearly periodic) spectra for flow separation lip noise is given by Eq. (3) for all angles.

$$f_p = S_t V/t \quad (3)$$

The Strouhal number, S_t, is 0.22 for the partial-span splitter plate lip geometries shown on Fig. 10 at all angles. The coaxial nozzle had a Strouhal number of 0.2. The Strouhal number is a weak function of the plate width (or circumference) and the velocity ratio as shown by the previous data. For example, the Strouhal number is 0.28 for the 40 cm wide plate shown on Fig. 11.

The agreement between the previous splitter plate and coplanar coaxial nozzle lip data with values predicted by Eq. (2) is discussed next. According to Eq. (2) the aeolian tone dipole noise term will dominate near $\theta_i = 90^o$, so that the $OASPL_c$ at that angle will be proportional to V^6. The data for the coaxial nozzle and splitter plate plotted on Figs. 6 and 18 agree with this result. Eq. (2) also indicates that the $OASPL_c$ will be proportional to V^5 near the inlet ($\theta_i = 20^o$), where the trailing edge noise term dominates. Although not shown directly herein, the data do follow the V^5 law at $\theta_i = 20^o$.

The shape of the radiation pattern was not affected by the lip thickness, lip width, or velocity ratio; but the level was affected (through the term ξ) as described by Eq. (2).

As shown before (Fig. 19), the shape of the radiation patterns for the splitter plate (at $\phi = 0^o$) and co-axial nozzle are the same, which is also indicated by Eq. (2). The data from Figs. 8 and 19 for these velocities are overlayed on Fig. 23 with one data point (at V = 152 m/sec, and $\theta_i = 90^o$) from each figure coinciding. A constant value of the parameter K (0.5 sec/m) was

used in Eq. (2) to calculate the radiation pattern shapes for the splitter plate and coplanar coaxial nozzle geometries. These analytical patterns are plotted on Figs. 7 and 18. The patterns were calculated relative to the common data point at $V = 152$ m/sec and $\theta_i = 90^o$. Eq. (2) describes the shape of the patterns very well for $\theta_i \leq 110^o$. Refraction causes the discrepancy for $\theta_i > 110^o$. Refraction which redirects the sound waves away from the jet axis, increases with frequency and velocity. Since the frequency of the lip noise is proportional to the velocity the discrepancy between the theory and the data will increase sharply with increases in velocity.

Data for the azimuthal variation of the noise for the splitter plate geometry fits the theoretical pattern, $\Phi = \cos^2\phi$, at $\theta_i = 90^o$ (fig. 9). And the shape of the polar radiation pattern, $OASPL_c<\phi_i>$, is independent of ϕ, which verifies neglecting a drag-dipole term in equation (2).

Additional understanding can be obtained by comparing results from Eqs. (2) and (3) to the data for the coaxial nozzle, where the core nozzle lip was extended to various lengths, L_c (Fig. 3(b)). Data for the effect of L_c on the flow separation lip noise is shown on Fig. 24 for a velocity ratio of one ($V_o/V = 1$). The core nozzle extension lengths were $L_c/d_c = 0$, 5, and 11. The turbulence is low and the velocity profiles were uniform for the coplanar nozzles case ($L/d_c = 0$). A significant turbulent boundary layer builds up along and in the extension pipe ($L_c/d_c = 5$, 11) and the outer and core nozzle velocity profiles at the extended core nozzle exit plane are nonuniform. However, the peak velocity of the outer nozzle velocity profile at the core nozzle exit plane, V_E decayed only slightly ($V_E/V_o \cong 1$, see the table on Fig. 23) even for the longest extension. Therefore, Fig. 24 contains a qualitative comparison that shows the effect of a nonuniform velocity profile on lip noise.

The lip noise spectra (frequency and shape) were about the same as for the coplanar nozzle ($L_c/d_c = 0$) at all angles, θ_i. In other words the spectral shape and frequency of this tone-like noise was essentially independent of L_c and θ_i as indicated by Eq. (3). The shape of the radiation pattern for the coplanar coaxial nozzle ($L_c/d_c = 0$) is the same as for the coaxial data in Fig. 19. There was, however, a significant change in the shape of the radiation pattern with an increase in L_c, as shown by the data points in Fig. 24.

Eq. (2) is now used to explain the difference in the shape of the radiation pattern caused by increasing L_c. One of the two noise sources in Eq. (2) is the trailing edge noise source. The radiation pattern for this source is given by $V^5 \cos^2(\theta_i/2)$, which is the dominant term in Eq. (2) when θ_i is small. The data in Fig. 24 shows that the $OASPL_c$ at small θ_i did not change with L_c. Therefore, a single curve for the radiation pattern of the trailing edge noise source would apply for all L_c. A dashed curve for $V^5 \cos^2(\theta_i/2)$ has been drawn on Fig. 24. The level of the data near 90^o changes when L_c/d_c changes from 0 to 5. The dipole term is dominant near 90^o, therefore, the level of the dipole term should vary with changes in L_c. The level of the dipole term is varied by using different values of K for each L_c/d_c as noted on Fig. 24 by the dash-dot curves ($K = 0.05$ for $L_c/d_c = 0$ and $K = 0.002$ for $L_c/d_c = 5$ and 11). The log sum of the trailing edge noise term and the dipole term appropriate for each L_c is the total noise predicted by Eq. (2) (solid curves on Fig. 24). The agreement between the theoretical curves and the data is good for $\theta_i < 100^o$. The discrepancy between the data and Eq. (2) for $\theta_i \geq 100^o$ is due to refraction of this high frequency noise.

The reduction in the level of the dipole source in going from $L_c/d_c = 0$ to 5 may be caused by the difference between the velocity gradient at the nozzle surfaces just upstream of the lip for these two lengths. The velocity profile was uniform for $L_c/d_c = 0$, which would result in a large gradient. There is a thick boundary layer for $L_c/d_c = 5$, which would result in a much smaller gradient.

Data on Fig. 24 were for a velocity ratio across the lip of unity. The high frequency tone-like lip noise disappeared for the extended core cases when the velocity ratio was below 0.5, just as it does for the coplanar coaxial nozzle.

Noise from Flow Separation Off Other Nozzle Surfaces

A flow separation region is a volume of fluid attached to the surface where the flow direction becomes reversed, forming vortices and wakes. Such regions can occur at any blunt or poorly designed nozzle surface such as a plug centerbody, the outer surface of an extended core nozzle of a coaxial nozzle, or a thick plate orifice nozzle. A flow separation region can also occur at some flow conditions at the outer wall of the mixing chamber formed by extending the outer nozzle of a coaxial nozzle. Poor ventilation of multitube nozzles has the same effect. Any degree of flow separation will cause some thrust loss and can also generate significant additional noise, beyond the basic jet noise of the nozzle. The noise from the nozzles listed above, all of which have regions of flow separation, will be discussed herein in order to tie in the Ref. 3 results with the new data contained. It is hoped that these few examples will impress upon the reader the importance of using nozzle designs that have no flow separation in jet noise experiments. No correlation will be made of these limited data, but it will be clear that the character of the noise (due to flow separation) for these nozzles will be somewhat different from the noise associated with the thin blunt lip discussed previously.

Plug nozzles. This section considers the noise generated by flow separation off the surface of the plug centerbody of a nozzle. Two plug centerbodies, each with a different degree of flow separation, are compared at the same velocity to plugs that exhibit little or no flow separation. The first comparison involves a sharply tapered plug with mild flow separation. The next comparison involves a blunt ended plug that exhibits strong flow separation. This plug is then installed in a coaxial nozzle to show that the suppression capability of this type of suppressor (i.e., the coaxial nozzle) can be seriously limited by flow separation noise.

Consider the plug nozzle geometries sketched on Fig. 25. The plug with the sharp taper is somewhat typical of an engine plug. If the plug is poorly designed there would be some flow separation

at the surface of the plug. In Fig. 25, the sound power level spectra for this plug nozzle (dashed line) is compared to the spectral data for the gradually tapered plug nozzle which has no flow separation (solid line). The data curves for these plug nozzles, which are the same size, are compared at two velocities. This comparison shows that even a fairly small degree of flow separation can produce significant noise that adds to the basic jet noise with substantially no flow separation. This result differs from the previous results where there was a narrow region of flow separation downstream of a relatively thin lip, in two important ways. The noise spectra caused by flow separation from the plug is as broadband as the jet noise. Furthermore, this additional noise follows the V^8 law and has about the same radiation pattern shape as jet noise, contrary to the results for the thin lips previously discussed.

Now consider the blunt and streamlined plug centerbodies sketched on Fig. 26, that are installed in a coaxial nozzle. These two plugs are compared on Fig. 26 at the same velocity ratios, velocity and plug and nozzle size. The sound pressure level spectra at 90^o that was obtained with a conical plug, having no flow separation (solid curves) is compared to that obtained from a blunt end plug with considerable flow separation (dashed curves). At a velocity ratio of 0 (VR = 0) there is no flow through the outer nozzle so that the comparison is essentially the same as the one just completed in Fig. 25. However, the flow separation with the blunt ended plug is stronger, which results in relatively more additional noise. The spectra of the flow separation noise is again as broadband as the jet noise; and again the noise follows the V^8 law and the radiation pattern is the same as jet noise. A similar comparison with a blunt plug was made in Ref. 3; the results were equivalent.

The effect of the outer nozzle flow is also shown on Fig. 26. As stated above the flow separation noise is broadband and significant for this case at all frequencies. At VR = 1 the jet noise from the outer nozzle stream dominates the flow separation noise, except at high frequencies. The high frequency part of this spectra is the most important when these results are scaled up to a full sized nozzle.

At the maximum jet noise suppression condition (VR = 0.5) the additional high frequency flow separation noise dominates the jet noise. The flow separation noise was unchanged at high frequency in going from VR = 0 to 0.5. Therefore, the noise suppression expected, based on pure coaxial jet noise, at VR = 0.5 was not observed because of flow separation noise. If the plug with mild separation (Fig. 25) had been used the suppression would still have been limited, but not so severely.

Convergent nozzles. The noise generated by circular nozzles with different inlet and lip shapes is shown on Fig. 27. The sound power level spectra for these nozzles is compared at the same jet velocity and nozzle diameter. These data have been combined from data reported in Ref. 3 in order to illustrate two points about flow separation noise. The data for all the nozzles with no flow separation are within ±1/2 dB of the single curve shown (solid line) that was drawn through the data. All these nozzles followed the pure jet noise laws for a large range of subsonic jet velocities. Thus, pure jet noise results, which is independent of the nozzle inlet and lip shape for these nozzles that have no flow separation.

The thick plate orifice nozzle has a small region of flow separation which generates some additional noise at high frequency, as shown by the dashed curve on Fig. 27. The resulting shape of the noise radiation pattern for this orifice is the same as for the nozzles without flow separation; and the orifice also follows the V^8 law. The reduction in the low frequency noise may be due to the more rapid velocity decay of the jet issuing from this type of nozzle.

Mixed flow coaxial nozzle. Another example of flow separation caused noise (based on data taken in Ref. 4) is shown on Fig. 28. A coaxial nozzle with a mixing chamber formed by a straight outer nozzle extension pipe of length L_o d_o = 2 and 6 is sketched on Fig. 28. As the velocity ratio, V_o/V, is decreased from 1.0, the noise caused by flow separation from the thin core nozzle lip decreases and finally disappears below about VR = 0.5 (e.g., Fig. 22). Then, when the velocity ratio falls below 0.3, a large flow separation region develops at the surface of the outer nozzle extension pipe (see sketch on Fig. 28). According to Fig. 28 considerable low frequency additional noise was generated by the region of flow separation that exists at VR = 0.2 for L_o/d_o = 2 and 6. The frequency of the peak of this additional noise was 630 Hz when the length was L_o/d_o = 2 and 450 Hz when L_o/d_o = 6. This noise is probably not an organ pipe longitudinal oscillation because the frequency should have decreased from 630 Hz to about 200 Hz when the length was increased from L_o/d_o = 2 to 6.

Lip Noise with No Flow Separation

Early model-scale jet noise data and engine data implied there is an additional noise source at low velocities because the data did not follow the V^8 law. Several investigators (e.g., Refs. 1 and 2) conjectured the additional noise source may be associated with a turbulent airstream passing one side of the nozzle exit lip (classic lip noise). The origin and level of the turbulence required to generate significant classic lip noise was not stated. Model-scale jet experiments have some initial turbulence (i.e., turbulence at nozzle exit plane generated upstream); typically the turbulence intensity is less than 1 percent. Engines have a high level of initial turbulence (10 to 15 percent). The nozzles used in both types of experiments did not generally suffer from flow separation. It was initially thought that even the low level of initial turbulence could generate significant lip noise, which in turn caused the discrepancy from the V^8 law.

In the previous sections it was shown that a type of lip noise does exist, but it was generated by turbulence caused by flow separation. The flow separation is the result of bad nozzle design, not the result of the inherent initial turbulence. The purpose of this section is to show that the initial turbulence levels of model jets and engines do not generate sufficient lip noise to differentiate it from jet noise in the far field. This result will be demonstrated with two nozzles that have no flow separation (Fig. 3(c)). One nozzle, with a stand-

ard inlet shape and a short lip, has low intitial turbulence levels (1/2 percent). The other nozzle has a standard inlet and a long extension pipe attached to the lip. The theory of Ref. 2 indicated that classic lip noise would follow a $V^5 \cos^2(\theta_i/2)$ law, which would be at a maximum near the inlet ($\theta_i = 0^o$) and follow a V^5 law there. Near the inlet, jet noise is at a minimum and it nearly follows a V^8 law there. Therefore, the spectra and level of the noise for these two nozzles will be examined at $\theta_i = 20^o$ and at low velocity because classic lip noise must be evident there if it exists.

In Fig. 29 a plot is shown of the SPL spectra near the acoustically wrapped pipe inlet (at $\theta_i = 20^o$) of a model nozzle (0.32 cm blunt lip) for a number of velocities at a low initial turbulence level (about 1/2 percent). The same spectral shape curve has been put through the data at each velocity. No second spectral peak for lip noise is apparent at any frequency; and the noise nearly follows V^8, not V^5. The level and radiation patterns of the noise (OASPL as a function of θ_i), for these velocities also fit the pure jet noise theory by Goldstein.[8] In addition, it was shown in Fig. 27 that the shape of the lip and inlet of a convergent nozzle has no effect on the spectra at any angle provided there is no flow separation. This adds further evidence to the conclusion that classic lip noise does not affect the jet noise from a single-stream model-scale conical nozzle, where $V \geq 120$ m/sec and the initial turbulence levels are low.

In the case of the early model-scale jet noise data, the additional noise noted near the inlet at the lowest velocities was probably due to internal noise (e.g., valve noise) radiating through the pipe wall to the microphone nearest the inlet pipe where the jet noise is lowest. In a jet noise experiment the lowest velocity reported is usually when the OASPL at 90^o starts to diverge from the V^8 law. At this point the microphone nearest an unshielded inlet pipe, which is closer to the pipe than the nozzle exit plane, will pick up some valve noise.

The experiment described in Fig. 27 was also performed with an extended lip nozzle (i.e., a long pipe added to the lip of a convergent nozzle). In this case, the initial turbulence near the 0.32 cm thick blunt nozzle lip (i.e., pipe end) was high (about 10 percent near the pipe wall). In Fig. 30 it is shown that the spectra at $\theta_i = 20^o$ is fit by the same single peak spectral curve shape at each velocity. The noise follows the V^8 law, even at low velocities. The exit velocity profile is parabolic. Therefore, the jet noise is lower and the spectral shape is somewhat different than observed for the short lip nozzle (Fig. 29) with a uniform velocity profile, when they are compared at the same centerline (peak) velocity.

These results show that the classic lip noise caused by initial turbulence levels of up to 10 percent intensity do not generate sufficient lip noise to differentiate it from jet noise in the far field.

Also consider again the coaxial nozzle, with the extended core, where lip noise is caused by flow separation off the thin lip of the extended core nozzle shown in Fig. 24. When the core nozzle was long the trailing edge noise radiation pattern was observed, as predicted in the classic lip noise analysis of Refs. 1 and 2. As the outer nozzle velocity decreased below half the core velocity the eddies leave the lip in a much less periodic manner, and the lip noise due to this flow separation disappears. In the limit of no outer nozzle flow this experiment reduces to a single stream nozzle with no flow separation and therefore there is no lip noise.

Concluding Remarks

Wherever there is flow separation from a nozzle surface there is additional noise generated, relative to the jet noise. This noise, which is more apparent in small-scale nozzles than large, can be avoided by careful nozzle design that avoids any flow separation.

The nearly periodic noise caused by flow separation from the thin blunt lip of the core nozzle of a coaxial nozzle was fully investigated herein and the data explained herein. The frequency of this noise is described at all angles by a Strouhal number, based on lip thickness, of 0.2. The turbulence and acoustic spectra were similar. This noise can be described by the sum of two independent noise sources. One is essentially the dipole noise from aeolian tone theory while the other is similar to trailing edge noise. This flow separation causing noise disappeared when the outer nozzle to core velocity ratio fell below 0.5, because the turbulent eddies were no longer shed periodically.

A preliminary investigation of the noise generated by flow separation off other nozzle surfaces was also performed. The characteristics of the noise generated by these surfaces is different than the high frequency tonelike noise generated by flow separation from a thin lip. Flow separation from the outer surface of an improperly designed core nozzle or plug centerbody occurs at all flow conditions. Flow separation does not occur off any inner surface of a convergent nozzle except a thick plate orifice. It occurs in a mixed flow coaxial nozzle at certain flow conditions.

The suppression obtained with a suppressor nozzle (e.g., coaxial and multitube nozzles) can be limited by the noise caused by flow separation. Examples of several types of flow separation caused noise that can occur with coaxial and multitube nozzle suppressor configurations are listed in the preceding two paragraphs and described in the text.

Experiments were also performed to determine if additional noise is generated by a turbulent flow past one side of a nozzle lip in the absence of flow separation. The spectral acoustic data near the inlet of model circular nozzles having no flow separation were studied at low velocities (down to 120 m/sec) and at low and high initial turbulence levels. The results showed that there was no additional noise beyond the jet noise near the inlet or at any other angle.

Nomenclature

C constant, dB

c_o speed of sound in environment, m/sec

d	diameter of nozzle, m
d_c	core nozzle diameter, m
d_o	outer nozzle diameter, m
f_p	frequency of peak noise, Hz
K	constant, sec/m
L_c	length of core nozzle extension beyond outer nozzle, m
L_o	length of outer nozzle extension beyond core nozzle, m
OASPL	overall sound pressure level, dB
$OASPL_c$	OASPL of flow separation noise only (i.e., jet noise removed), dB
PWL	sound power level, dB (ref. 10^{-12} W)
R	microphone radius, m
SPL	sound pressure level, dB
SPL_c	SPL of flow separation noise only (i.e., jet noise removed), dB
SPL_p	SPL of peak noise, dB
S_t	Strouhal number based on lip thickness
t	lip thickness, m
u'	axial velocity perturbation, m/sec
V	jet velocity, m/sec
V_E	maximum velocity of outer nozzle stream at core exit plane, m/sec
V_{low}	low jet velocity on side of plate where flow restricted, m/sec
V_o	outer nozzle jet velocity, m/sec
VR	velocity ratio across lip outer/core for coaxial nozzle, or low/high splitter plate nozzle
w	splitter plate span or core nozzle circumference, m
x	distance downstream of splitter plate trailing edge, m
y	distance away from splitter plate edge (normal to plate plane), m
θ_i	polar angle from nozzle inlet, deg
ζ	correlation length, m
ρ_o	ambient density, g/m^3
Φ	$\Phi = 1/2$ for coaxial nozzle and $\Phi = \cos^2\phi$ for splitter plate nozzle
ϕ	azimuthal angle from plane perpendicular to plate, deg

References

1. Leppington, F., "Scattering of Quadrupole Sources Near the End of a Rigid Semi-Infinite Circular Pipe," ARC-CP-1195, Papers on Novel Aerodynamic Noise Source Mechanisms at Low Jet Speeds, Aeronautical Research Council, 1972.

2. Ffowcs Williams, J. and Gordon, C., "Noise of Highly Turbulent Jets at Low Exhaust Speeds," AIAA Journal, Vol. 3, Apr. 1965, pp. 791-793.

3. Olsen, W., Gutierrez, O., and Dorsch, R., "The Effect of Nozzle Inlet Shape, Lip Thickness and Exit Shape and Size on Subsonic Jet Noise," AIAA Paper 73-187, 1973, Washington, D.C.

4. Olsen, W.; Friedman, R.: Jet Noise from Coaxial Nozzles over a Wide Range of Geometric and Flow Parameters. AIAA Paper 74-43, 1974, Washington, D.C.

5. Brinich, P., Boldman, D., and Goldstein, M., "Vortex Shedding from a Blunt Trailing Edge with Equal and Unequal External Mean Velocities," TN D-8034, 1975, NASA.

6. Phillips, O., "The Intensity of Aerolian Tones," Journal of Fluid Mechanics, Vol. 1, Pt. 6, Dec. 1956, pp. 607-624.

7. Fink, M., "Prediction of Externally Blown Flap Noise and Turbomachinery Strut Noise," United Technology Research Center (NASA CR-134883; NAS3-17863), 1975, p. 56.

8. Goldstein, M., "Aeroacoustics," SP-346, 1974, NASA, pp. 219-230.

9. Ffowcs Williams, J. and Hall, L., "Aerodynamic Sound Generation by Turbulent Flow in the Vicinity of a Scattering Half Plane," Journal of Fluid Mechanics, Vol. 40, Pt. 4, Mar. 1970, pp. 657-670.

10. Mabey, D., "Analysis and Correlation of Data on Pressure Fluctuation in Separated Flow," Journal of Aircraft, Vol. 9, Sept. 1972, pp. 642-648.

11. Goldstein, M. and Howes, W., "New Aspects of Subsonic Aerodynamic Noise Theory," TN D-7158, 1973, NASA.

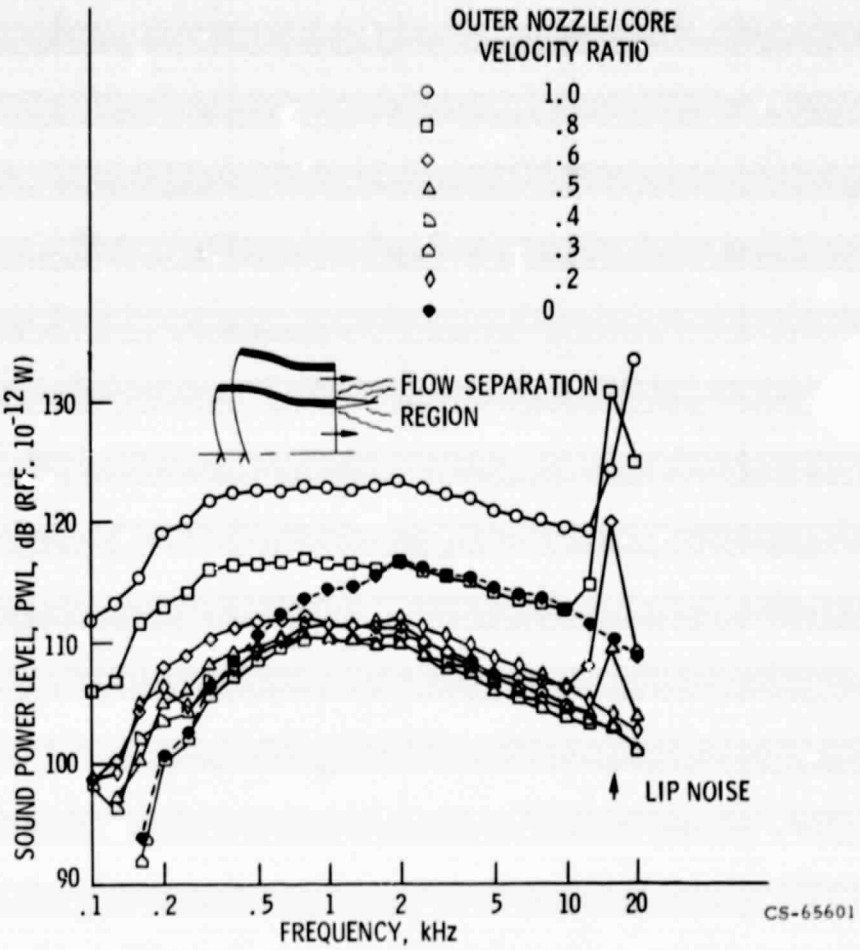

Figure 1. - Coaxial nozzle lip noise from ref. 3. Core velocity, 245 m/sec; core diam., 5.3 cm; area ratio, 5.4; lip thickness, 0.25 cm.

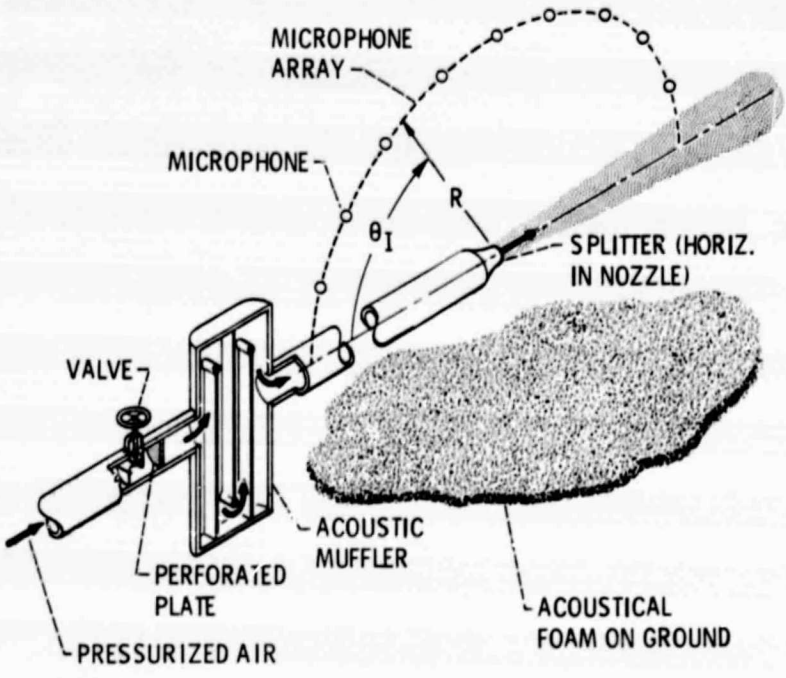

Figure 2. - Schematic sketch of flow system with microphone array for splitter nozzle tests.

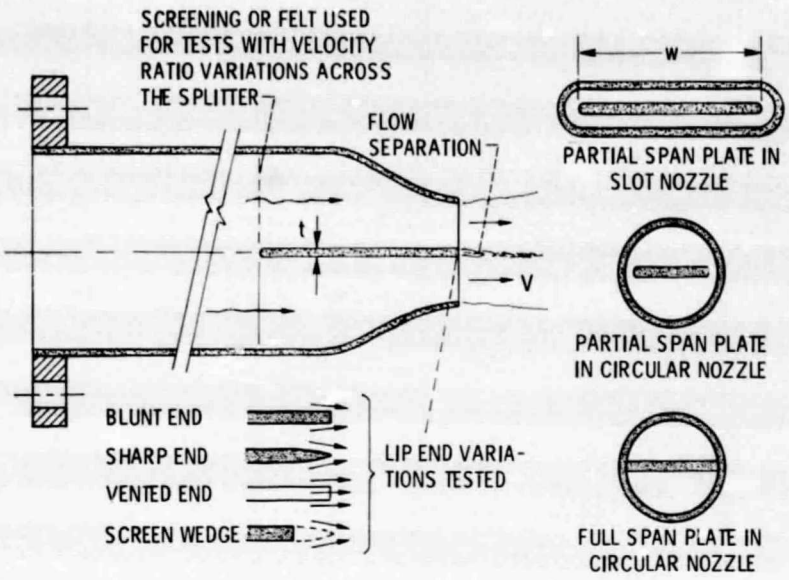

(a) NOZZLES WITH FLOW SEPARATION FROM SPLITTER PLATE.

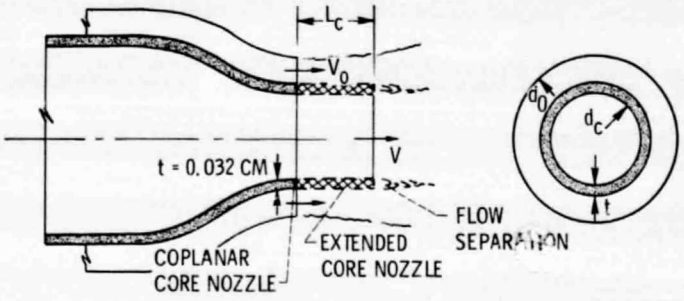

(b) COAXIAL NOZZLE WITH FLOW SEPARATION FROM CORE NOZZLE LIP.

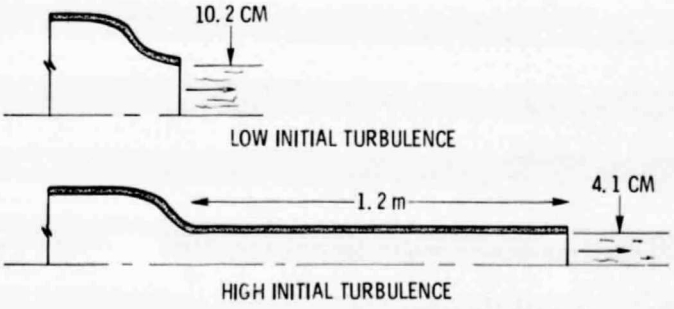

(c) CIRCULAR NOZZLES WITH NO FLOW SEPARATION.

Figure 3. - Sketches of nozzles extensively tested.

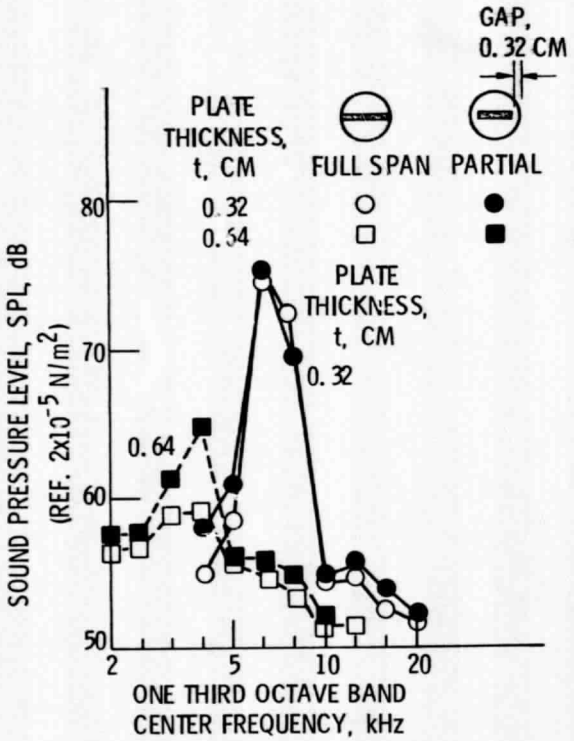

Figure 4. - Comparison of full span and partial span splitter plates. Angle, θ_i, 100^0; velocity, 91 m/sec; nozzle diameter, 7.6 cm; free field lossless data at 3 m; environmental temperature, 25 C.

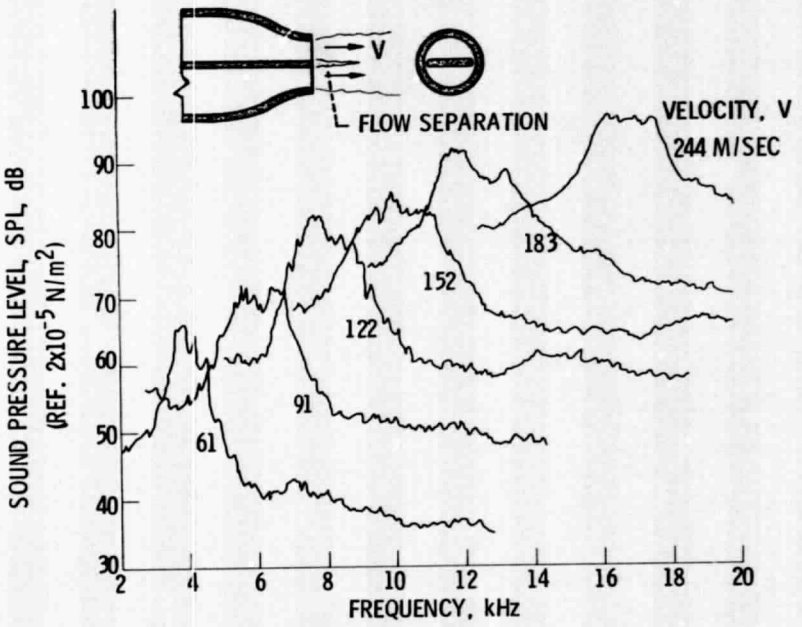

Figure 5. - Narrowband spectra of plate lip flow separation noise at several velocities. Plate thickness, 0.32 cm; plate span, 7.1 cm; nozzle diam., 7.8 cm; free field data at 3 m; polar angle, θ_i, 100^0; azimuthal angle, $\varphi = 0^0$; velocity ratio, 1.; environment temperature, 6 C; bandwidth 60 Hz.

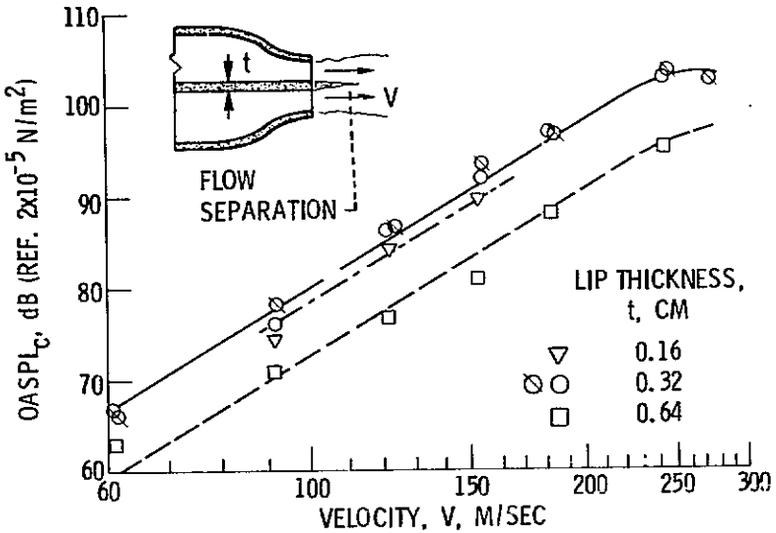

Figure 6. - Variation of the flow separation lip noise level, OASPL$_C$, with velocity for several splitter plate thicknesses. Partial-span splitter plate width, w, 7.1 cm; velocity ratio, 1.0; polar angle, θ_i, 100^0; azimuthal angle, φ, 0^0; free field lossless data at 3 m; environmental temperature, 25 C.

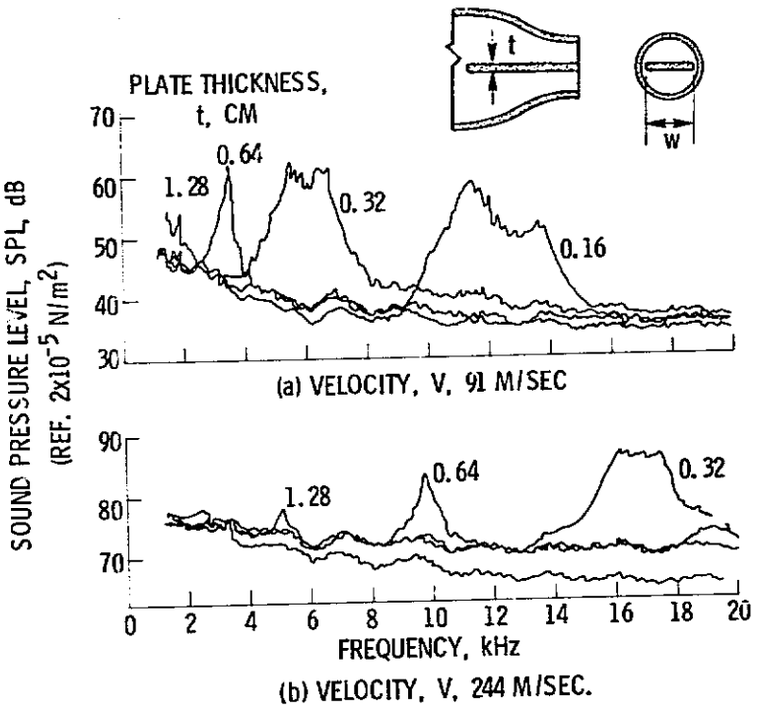

(b) VELOCITY, V, 244 M/SEC.

Figure 7. - Narrow band spectra for several plate lip thicknesses. Partial splitter plate span, w, 7.1 cm; nozzle diam., 7.8 cm; microphone angle, θ_i, 100^0; azimuthal angle, φ, 0^0; free field data at 3 m; velocity ratio, 1.0; environmental temperature 42^0 F; bandwidth 60 Hz.

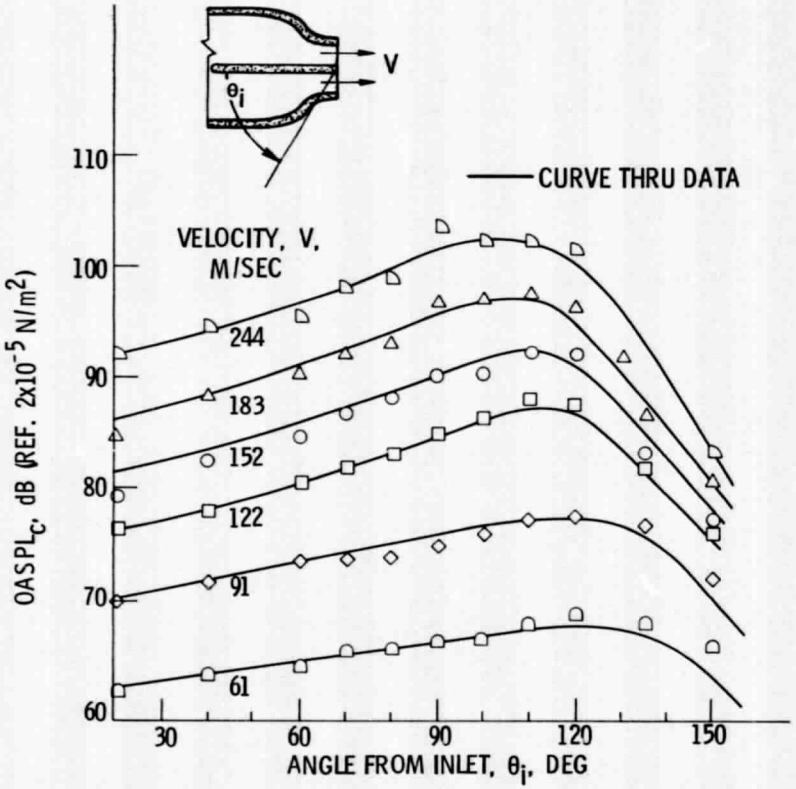

Figure 8. - Noise radiation pattern of flow separation lip noise, $OASPL_C$, for several velocities. Plate thickness, 0.32 cm; partial span splitter plate span, 7.1 cm; nozzle diam., 7.8 cm; free field lossless data at 3 m; azimuthal angle, φ, 0^0; velocity ratio, 1.0; environmental temperature, 25 C.

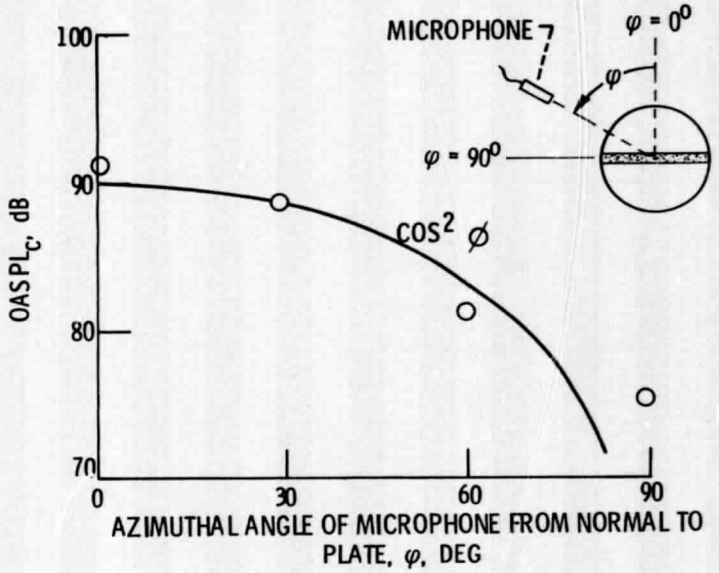

Figure 9. - Variation of $OASPL_C$ at $\theta_i = 90^0$ with azimuthal angle, φ. Plate thickness, 0.32 cm; velocity, 152 m/sec; velocity ratio, 1.0; full span splitter plate of span, 7.6 cm; free field lossless data at 3 m; environmental temperature, 25 C.

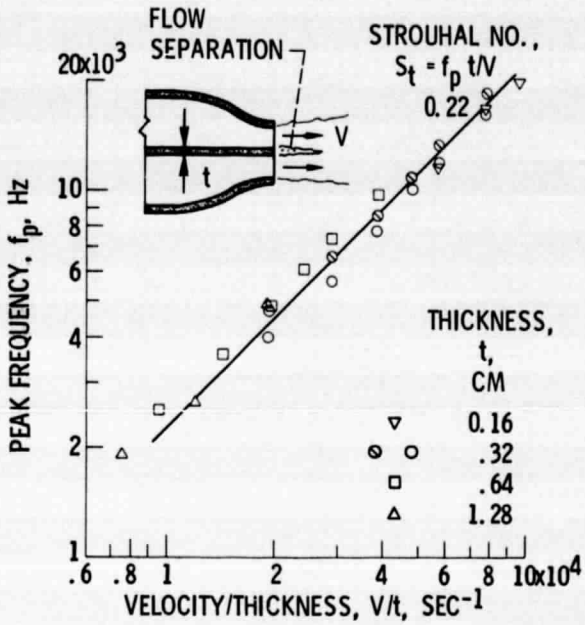

Figure 10. - Variation of peak frequency with velocity and plate thickness. Partial plate width, w, 7.1 cm; peak frequency determined from narrow band SPL spectra of 60 Hz bandwidth; velocity ratio, 1.

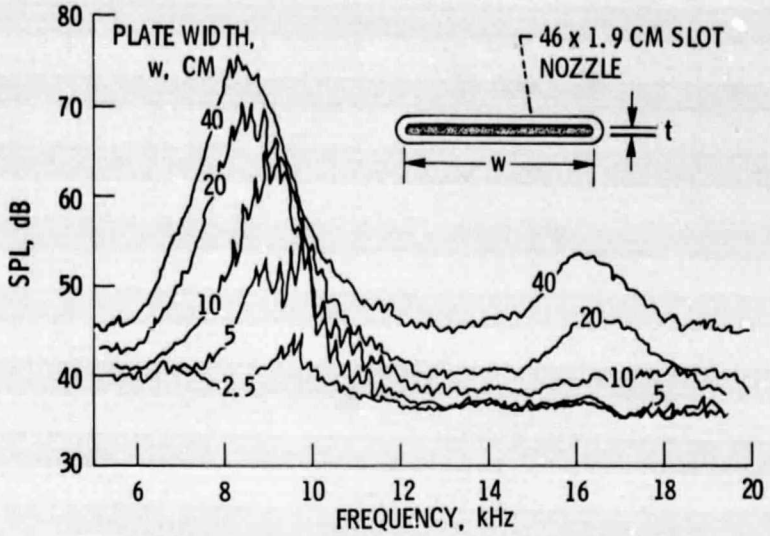

(a) NARROWBAND SPECTRA FOR SEVERAL PLATE WIDTHS, w, AT A VELOCITY OF 91 M/SEC.

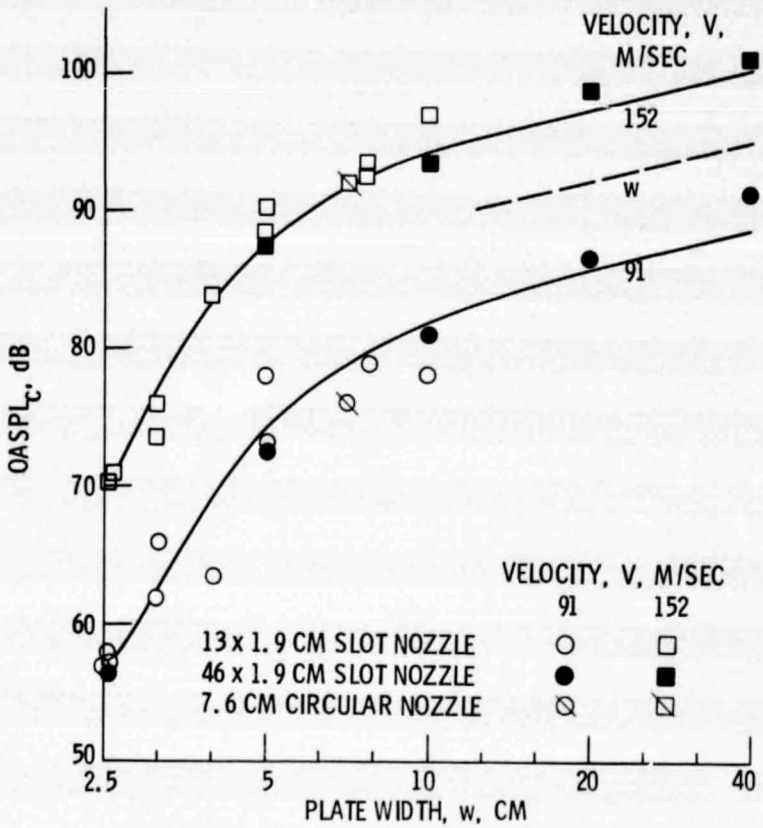

(b) VARIATION OF OASPL$_C$ WITH PLATE WIDTH, w, FOR SEVERAL VELOCITIES AND NOZZLES.

Figure 11. - Effect of splitter plate width, w, on flow separation noise from lip. Partial span splitter plate thickness, t, 0.32 cm; velocity ratio, 1.0; free field data at 3 m; polar angle, θ_j, 100^0; azimuthal angle, φ, 0^0; environmental temperature, 25 C.

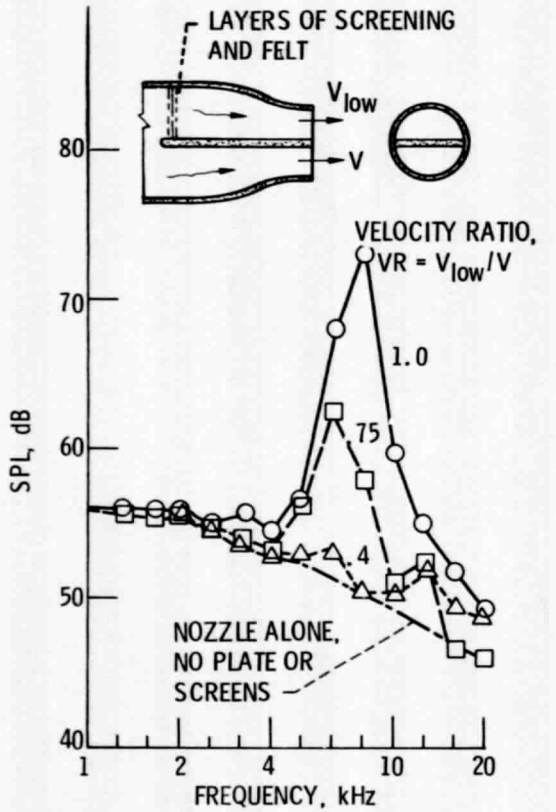

Figure 12. - Effect of velocity ratio across splitter plate. Plate thickness, 0.32 cm; width, 10 cm; velocity, V, 92.5 m/sec; microphone angle, θ_i, 90^0; azimuthal angle, φ, 0^0; free field lossless data at 4.6 m; environmental temperature 25 C.

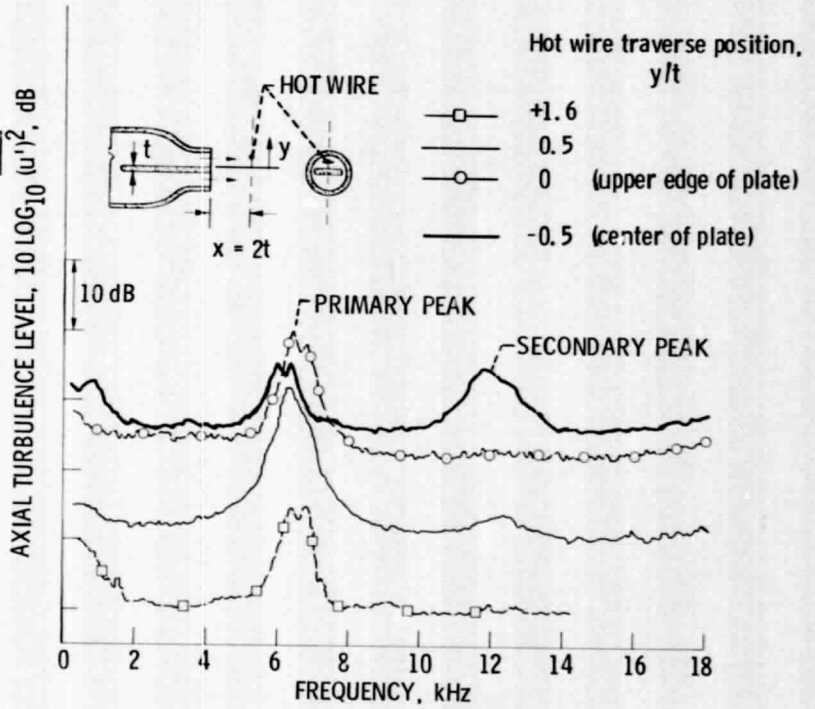

Figure 13. - Axial turbulent velocity spectra from hot wire at several traverse positions, y, across plate wake. Axial hot wire position, x = 2t; narrowband spectra of bandwidth, 60 Hz; velocity, 87 m/sec; velocity ratio, VR, 1.0; plate thickness, t, 0.32 cm; plate width, 7.1 cm.

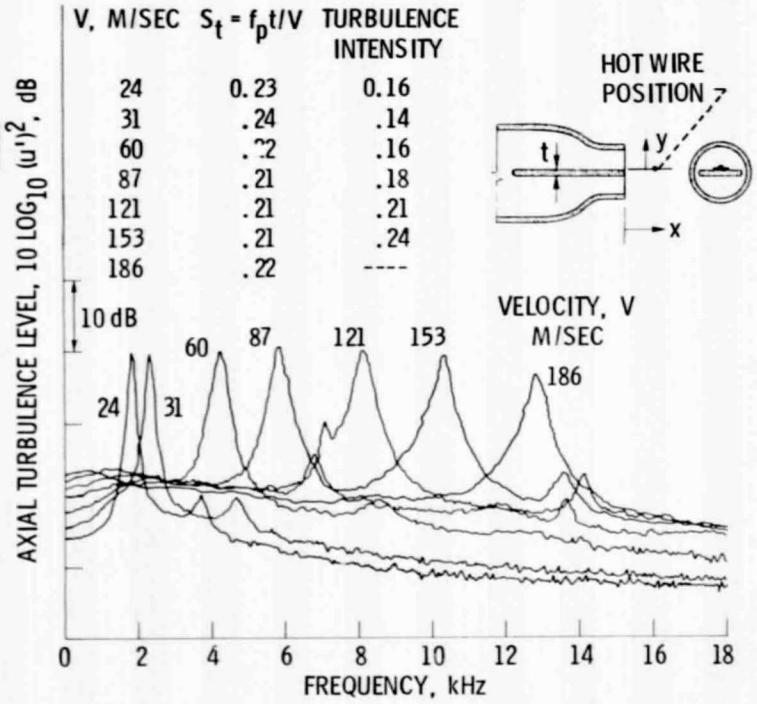

Figure 14. - Effect of velocity on axial turbulent velocity spectra. Narrowband spectra of bandwidth, 60 Hz; hot wire at position x = 2t and y = 0; partial span splitter plate thickness, t, 0.32 cm; width, 7.1 cm; velocity ratio, 1.0.

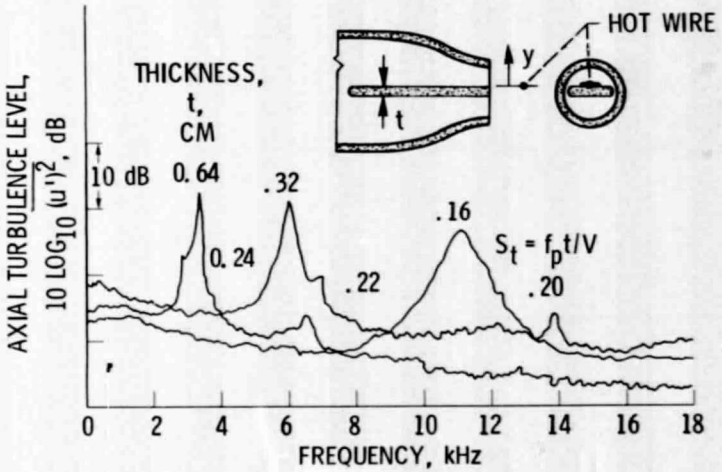

Figure 15. - Effect of plate thickness, t, on axial turbulent velocity spectra. Hot wire at x = 2t and top edge of plate (y = 0); narrowband spectra of bandwidth, 60 Hz; velocity, 87 m/sec; velocity ratio, 1.0; partial span splitter plate width, 7.1 cm.

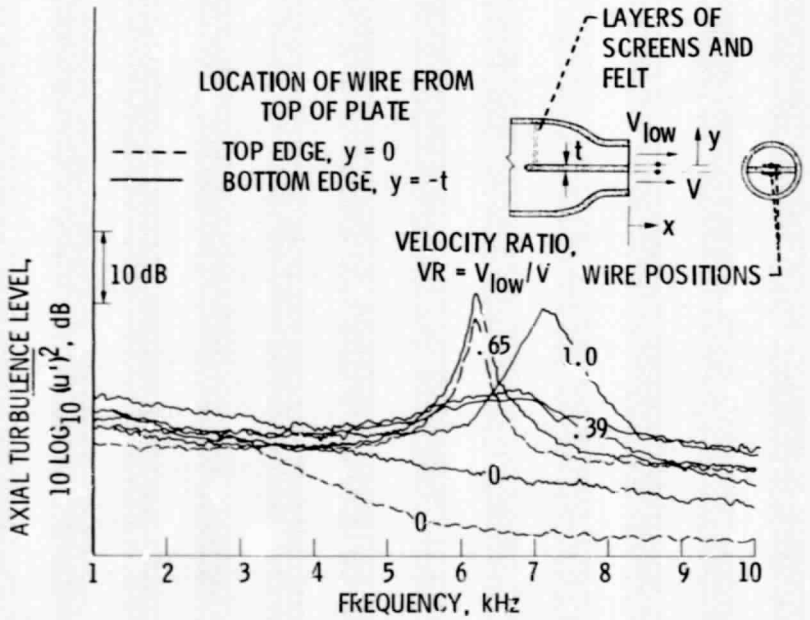

Figure 16. - Effect of velocity ratio, VR, on axial turbulent velocity spectra. Hot wire at x = 2t and both sides of plate (y = 0 and -t); narrowband spectra of bandwidth, 60 Hz; velocity, 87 m/sec; full span splitter plate thickness, t, 0.32 cm; width, 7.1 cm.

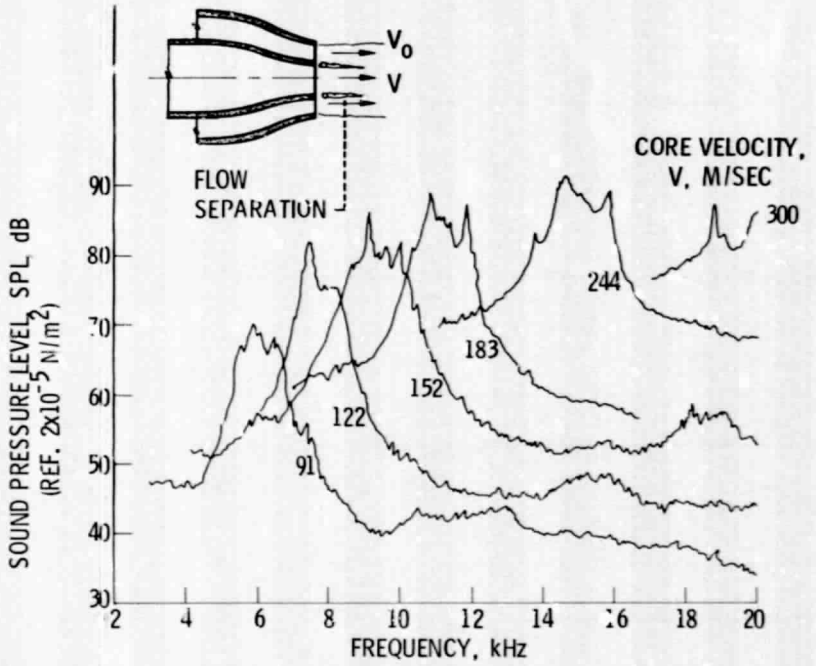

Figure 17. - Narrowband spectra for the coaxial nozzle core lip flow separation noise at several velocities. Velocity ratio, VR = V_o/V = 1; core nozzle lip thickness, 0.32 cm; core diameter, 5.3 cm; outer/core area ratio, 5.4; bandwidth, 60 Hz; free field data at 4.6 m; polar angle, 105^o; environmental temperature, 25 C.

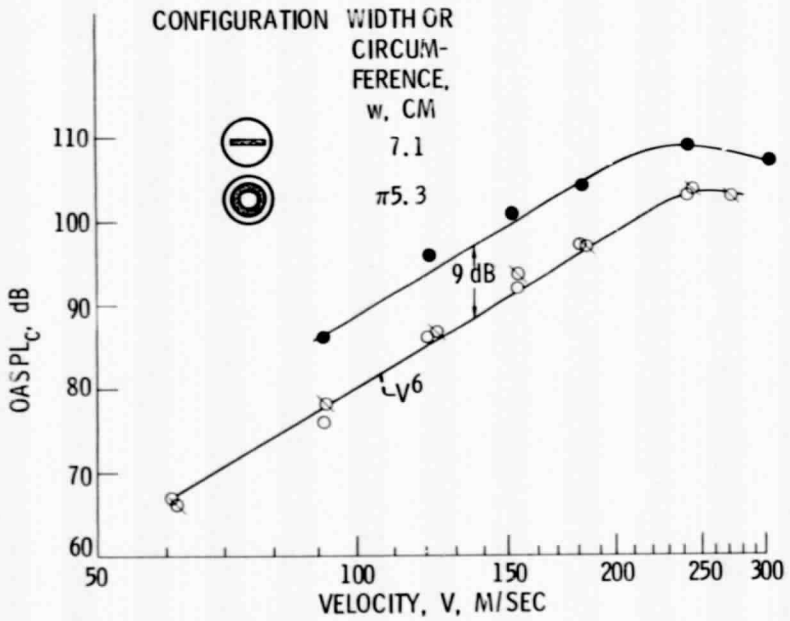

Figure 18. - Variation of flow separation lip noise level, $OASPL_c$, with velocity for the coaxial nozzle and splitter plate geometries. Lip thickness, t, 0.32 cm; velocity ratio, 1.0; polar angle, θ_i, 100°; free field lossless data scaled to 3 m distance and 25 C environmental temperature.

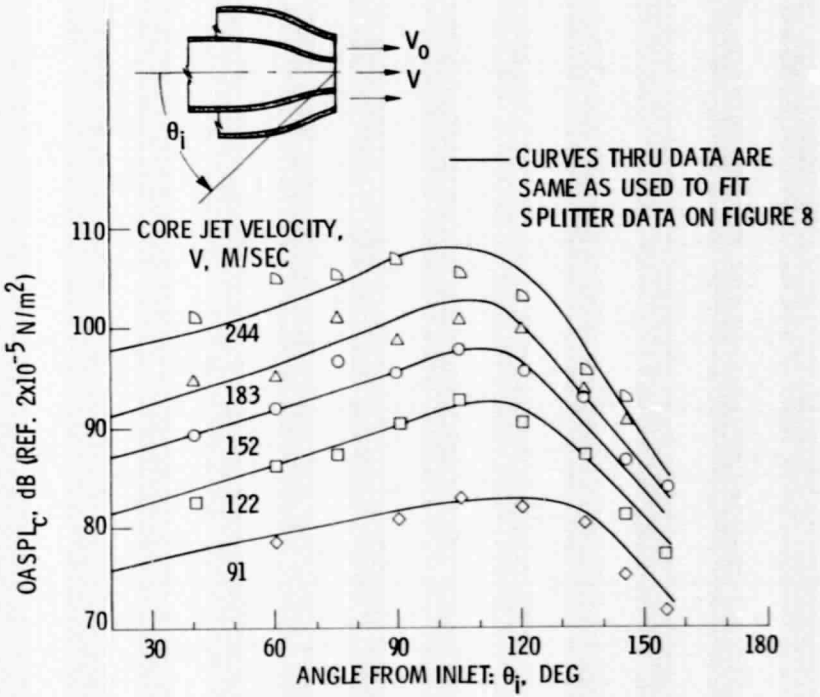

Figure 19. - Noise radiation pattern of the coaxial nozzle core lip flow separation noise, $OASPL_c$, for several velocities. Velocity ratio, 1; core nozzle lip thickness, 0.32 cm; core diam., 5.3 cm; outer nozzle diam., 13.4 cm; free field lossless data at 4.6 m; environmental temperature 25 C.

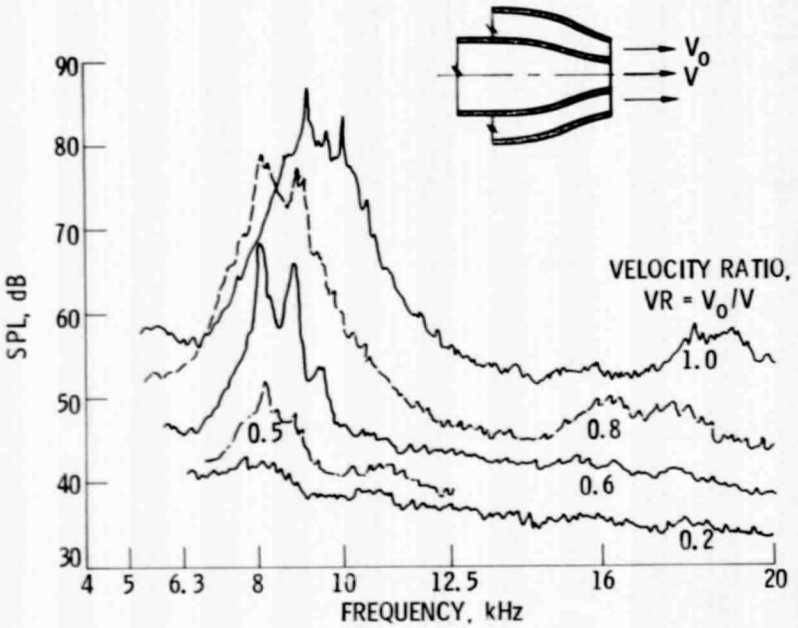

Figure 20. - Narrowband spectra for the coaxial nozzle core lip flow separation noise for several velocity ratios, VR. Core velocity, V, 152 m/sec; core nozzle lip thickness, 0.32 cm; core diameter, 5.3 cm; outer/core area ratio, 5.4; bandwidth, 60 Hz; free field data at 4.6 m; polar angle, 105°; environmental temperature, 25 C.

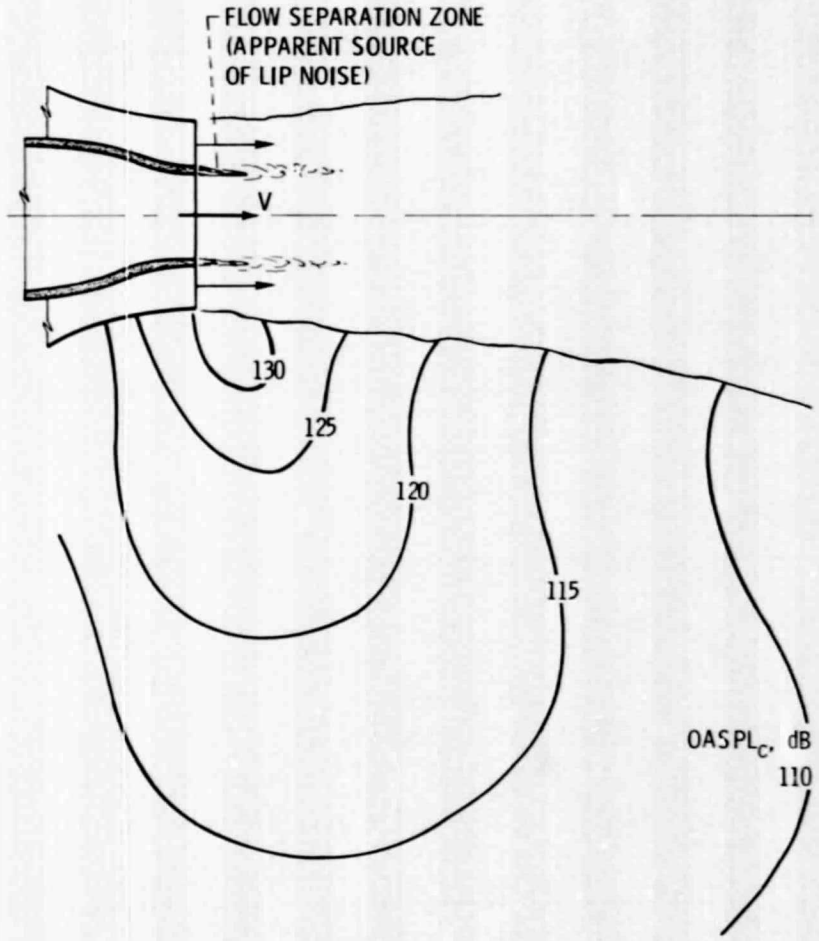

Figure 21. - Contour map of the $OASPL_C$ near the coaxial nozzle. Core velocity, V, 152 m/sec; velocity ratio, VR, 1.0; core nozzle lip thickness, 0.32 cm; core nozzle diameter, 5.3 cm; area ratio, 5.4.

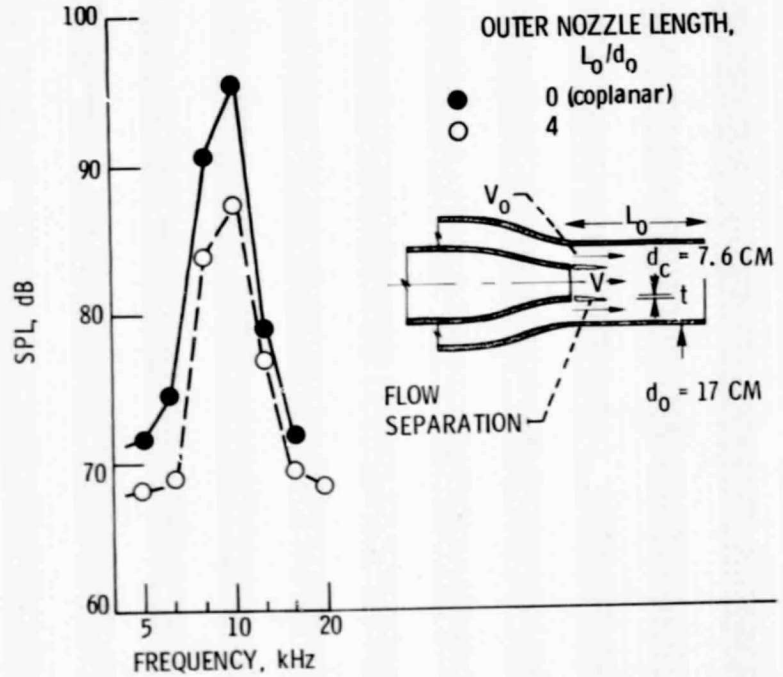

Figure 22. - Effect of extended outer nozzle on noise generated by flow separation at core nozzle lip. Core velocity, V, 152 m/sec; core lip thickness, t, 0.32 cm; velocity ratio, V_o/V, 1.0; polar angle, θ_i, 105^0; free field lossless data at 4.6 m.

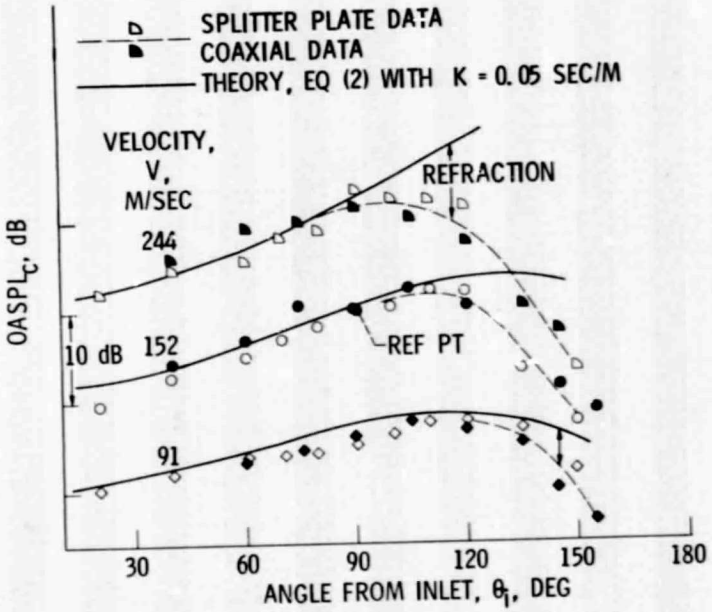

Figure 23. - Comparison of data and theoretical prediction for the shape of the radiation patterns at several velocities. Figure 7 (splitter data) and figure 18 (coaxial data) were overlayed so that the data points at V = 152 m/sec and $\theta_i = 90^0$ coincided.

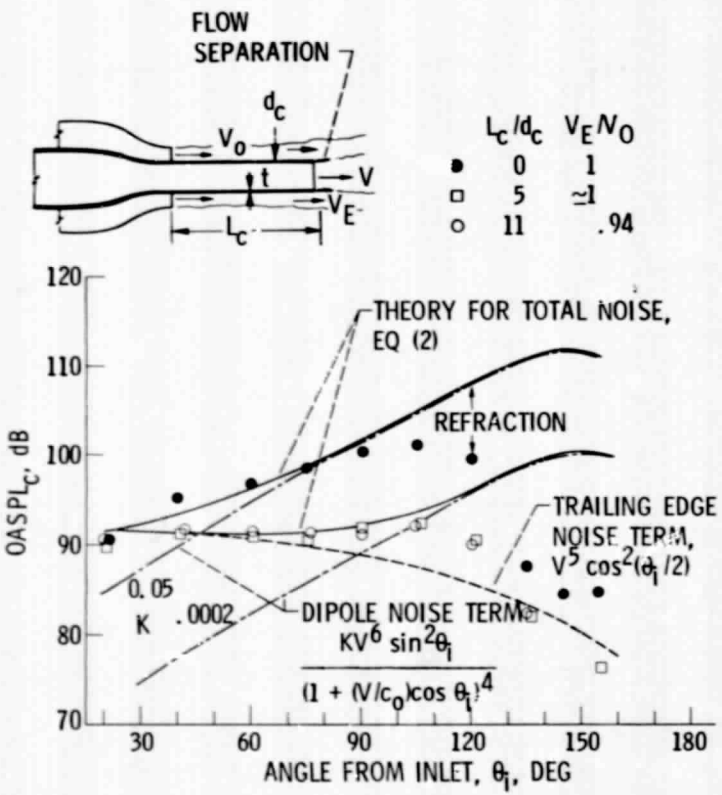

Figure 24. - Comparison of data and theory for the shape of the lip noise radiation pattern of an extended core nozzle lip coaxial nozzle. Core center line velocity, V, 244 m/sec; velocity ratio, V_o/V, 1.0; lip thickness, t, 0.25 cm; core diameter, d_c, 5.3 cm; outer nozzle diameter, 13.5 cm; free field lossless data at 4.6 m from core exit.

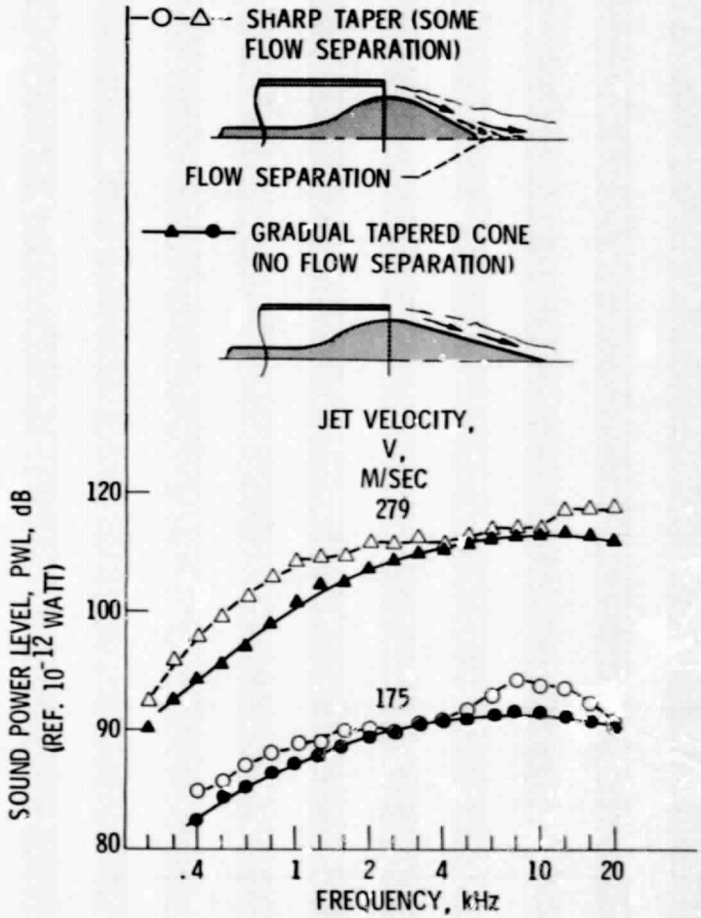

Figure 25. - Effect of some flow separation off plug on noise generation. Nozzle diameter, 10.3 cm; maximum plug diameter 9.3 cm; free field lossless data; environmental temperature, 25 C.

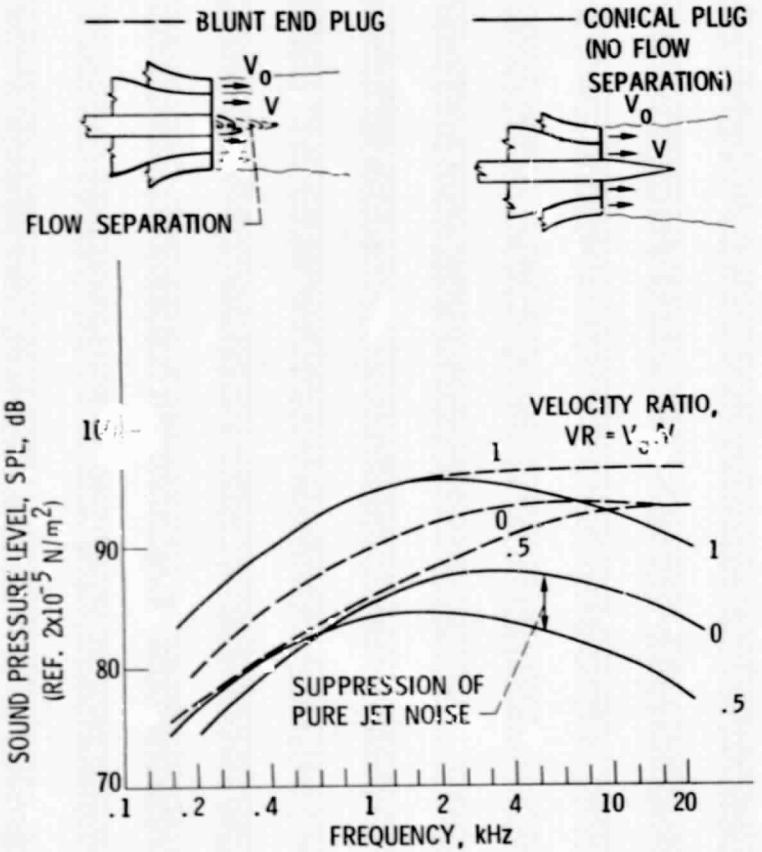

Figure 26. - Effect of flow separation on noise spectra for a coaxial nozzle with a plug centerbody. Coaxial nozzle area ratio, 3.34; core diameter, 10 cm; plug diam., 7.1 cm; core velocity, V, 300 m/sec; ambient temp., 25 C; free field lossless data at 4.6 m and $\theta_i = 90^0$.

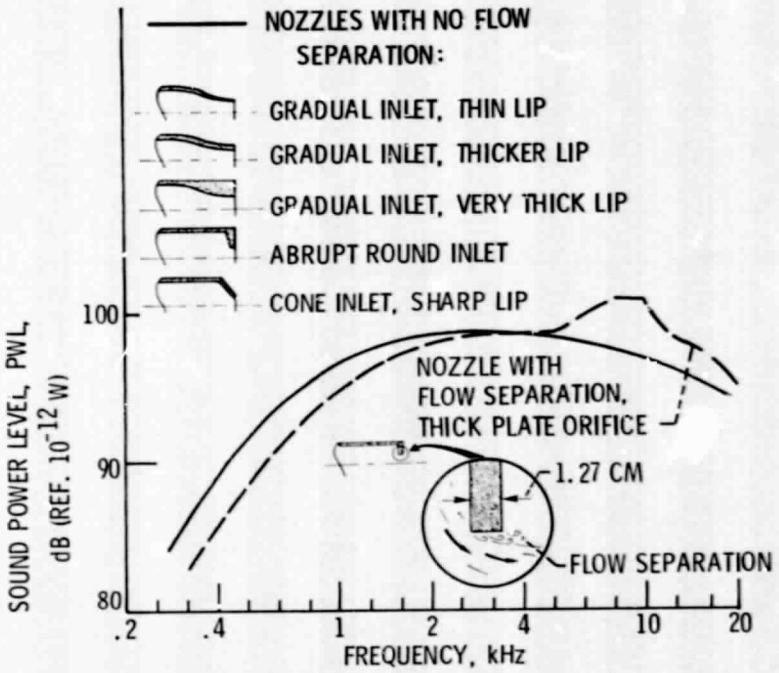

Figure 27. - Effect of nozzle inlet and lip shape. Nozzle diameter, 4.1 cm; jet velocity, 239 m/sec; data corrected to free field.

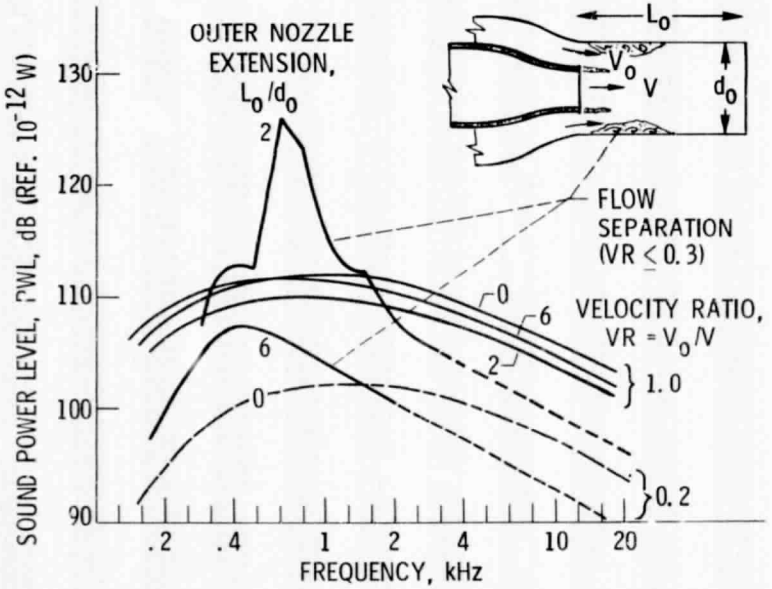

Figure 28. - Effect of flow separation off extended outer nozzle wall on coaxial nozzle noise. Core nozzle dia. 6 cm; outer nozzle/core area ratio, 3.9; core velocity, V, 225 m/sec; environmental temperature, 25 C; free field lossless data at 4.6 m radius.

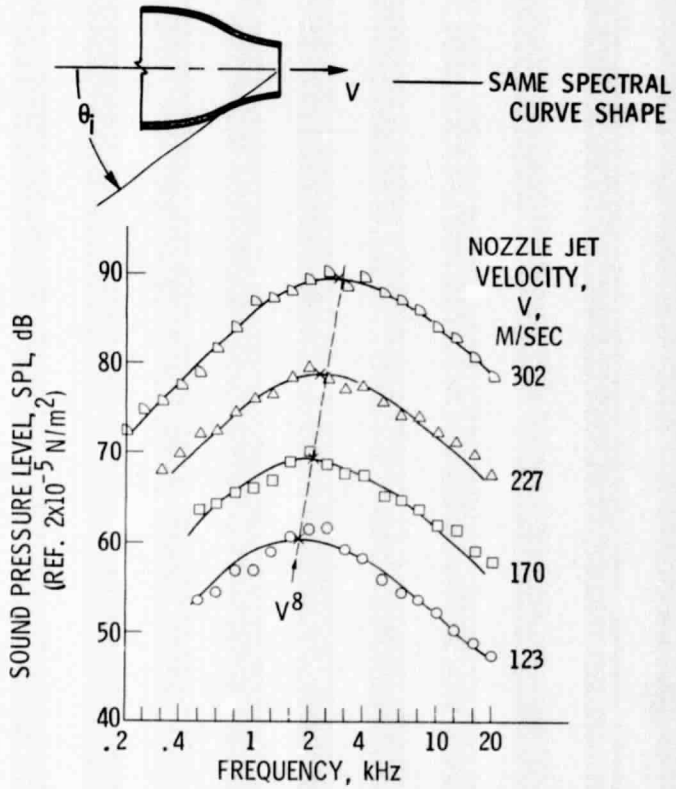

Figure 29. - Jet noise spectra at $\theta_j = 20^0$ for a nozzle with low initial turbulence (1/2%). Convergent nozzle diameter, 10 cm; free field lossless data at 4.6 m; inlet pipe acoustically wrapped; environmental temperature, 25 C; lip thickness, 0.32 cm.

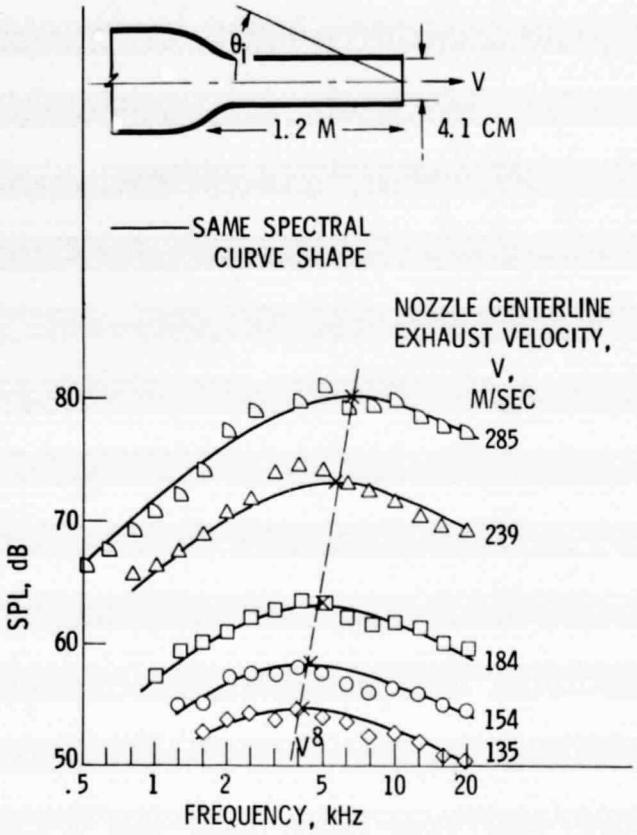

Figure 30. - Jet noise spectra at $\theta_i = 20^0$ for a nozzle with high initial turbulence (10% at wall). Nozzle diameter, nozzle lip extension, 1.2 m; free field lossless data at 3 m; inlet pipe acoustically wrapped; environmental temperature, 25 C; lip thickness, 0.32 cm.